

UNIVERSIDAD DE SEVILLA
FACULTAD DE MEDICINA
DEPARTAMENTO DE MEDICINA



Non-invasive diagnosis of non-alcoholic fatty liver disease

TESIS DOCTORAL

Rocío Gallego Durán

Unidad de Gestión Clínica de Aparato Digestivo Intercentros de los Hospitales Universitarios
Virgen Macarena- Virgen del Rocío, Sevilla.

Instituto de Biomedicina de Sevilla (IBiS).

Centro de Investigación Biomédica en Red de enfermedades hepáticas y digestivas
(CIBERehd)

D. MANUEL ROMERO GÓMEZ,
CATEDRÁTICO DE MEDICINA DEL DEPARTAMENTO DE
MEDICINA DE LA UNIVERSIDAD DE SEVILLA

CERTIFICA:

Que la Tesis Doctoral que lleva por título: “Non-invasive diagnosis in non-alcoholic fatty liver disease”, presentada por Doña Rocío Gallego Durán para optar al grado de Doctor con Mención Internacional, ha sido realizada en el Departamento de Medicina de la Facultad de Medicina de la Universidad de Sevilla.

Revisado el texto, doy mi conformidad para su presentación y defensa para optar al grado de Doctor con Mención Internacional por la Universidad de Sevilla.

Fdo. Prof. Manuel Romero Gómez

Director y tutor de la tesis doctoral

21 Marzo 2017

List of abbreviations in order of appearance

NAFLD: Non-alcoholic Fatty liver disease

NASH: Non-alcoholic steatohepatitis

SS: Simple steatosis

AUROC: Area under the receiver operating characteristic curve

PNPLA3: patatin-like phospholipase domain containing 3

TM6SF2: transmembrane 6 superfamily 2

FGF21: fibroblast growth factor 21

HCV: Hepatitis C virus

SRTR: Scientific Registry of Transplant Recipients

Mm: Millimetres

CRP: C-reactive protein

TNF- α : Tumour necrosis factor alpha

FFAs: Free fatty acids

ROS: Reactive oxygen species

IR: Insulin resistance

GGT: Gamma-glutamyl transpeptidase

AST: Aspartate transaminase

ALT: Alanine transaminase

NAS Score: NAFLD Activity Score

SAF Score: Steatosis Activity and Fibrosis Score

NASH-CRN: NASH Clinical Research Network

NIH: National Institutes of Health

US: Abdominal ultrasound

CT: Computed tomography

MRI: Magnetic resonance imaging

PDFF: Proton density fat fraction

MRE: Magnetic resonance elastography

MRS: Magnetic resonance spectroscopy

TE: Transient elastography

CAP: Controlled attenuation parameter

ARFI: Acoustic Radiation Force Impulse

CK-18: Cytokeratin-18

mRNA: Messenger RNA

NFS: NAFLD Fibrosis Score

PPV: Positive predictive value

NPV: Negative predictive value

APRI index: AST to Platelet Ratio Index

UPLC-MS: ultraperformance liquid chromatography coupled to mass spectrometry

GWAS: Genome-wide associations studies

SNPs: Single nucleotide polymorphisms

HTGC: Hepatic triglyceride content

¹H-MRS: proton magnetic resonance spectroscopy

CRF: Case report form

BMI: Body mass index

HDL-c: High-density lipoprotein cholesterol

LDL-c: Low-density lipoprotein cholesterol

Rpm: Revolutions per minute

ELISA: Enzyme-linked immunosorbent assay

SSFSE-T2: Single Shot Fast Spin Echo T2-weighted

FAST-STIR: Fast Short inversion Time Inversion Recovery

inPHASE-outPHASE: In and out Phase

FoV: Field of view

Sec: Seconds

Px: Pixels

qRT-PCR: Quantitative real-time polymerase chain reactions

RIN: RNA Integrity number

SD: Standard deviation

ROC: Receiver operating characteristics

OR: Odds ratios

kg/m²: Kilograms per square meter

Se: Sensitivity

SP: Specificity

mmol/L: Millimoles per litre

IU/L: International units per litre

mg/dL: Milligrams per decilitre

g/dL: Grams per decilitre

kPa: Kilopascals

ng/ml: Nanograms per millilitre

GE: General Electrics

INDEX

1. BACKGROUND	14
1.1 Non-alcoholic fatty liver disease concept, epidemiology, comorbidities, complications, and pathophysiology	16
1.2 Management and care of patients with NAFLD	20
1.3 Current diagnosis: liver biopsy assessment	22
1.4 Non-invasive diagnosis of NAFLD	25
1.4.1. Imaging biomarkers	28
1.4.2. Serum biomarkers	31
1.4.3 Genetic and epigenetic biomarkers	34
2. HYPOTHESIS	38
3. AIMS	41
4. RATIONALE	44
5. MATERIAL AND METHODS	47
5.1 Patients, inclusion and exclusion criteria and ethical aspects of the research	49
5.2 Clinical, anthropometric and biochemical measurements	50
5.3 Histological staging and grading	51
5.4 Imaging biomarkers	53
5.4.1 Study design and patients.....	53
5.4.2 Magnetic resonance image acquisition	54
5.4.3 MR imaging processing to define NASHMRI and FibroMRI imaging biomarkers.....	55
5.4.3.1 Development and standardisation of imaging biomarkers.....	55
5.4.3.2 Validation of imaging biomarkers	58
5.4.4 Comparison with biochemical biomarkers and transient elastography	58
5.5 Genetic and epigenetic biomarkers	59
5.5.1 Patients and study design	59
5.5.2 DNA isolation, quantification and single-nucleotide polymorphisms genotyping	59

5.5.3 Evaluation of FGF21 liver expression and peripheral mononuclear blood cells	60
5.5.4 Liver microRNAs isolation and quantification	60
5.5.5 Serum microRNAs isolation, quantification, and analysis	63
5.6 Statistical analyses	65
5.6.1 Imaging biomarkers analysis	65
5.6.2 Genetic and epigenetic analysis	66
6. RESULTS	67
6.1 Imaging biomarkers	69
6.1.1 Development and standardisation of NASHMRI to detect steatohepatitis.....	69
6.2.2 Definition of FibroMRI for significant fibrosis prediction.....	72
6.2.3. Comparative analyses of NASHMRI and FibroMRI.....	74
6.2.3.1 Standardisation of NASHMRI and FibroMRI across MRI systems.....	74
6.2.3.2 Comparative analysis with non-invasive biochemical markers of steatohepatitis.....	75
6.2.3.3 Comparative analysis with non-invasive biochemical markers of significant fibrosis.	76
6.2 Genetic and epigenetic biomarkers	78
6.2.1 Hepatic FGF21 expression is increased in NASH patients.....	78
6.2.2 Serum FGF21 levels are increased in advanced NAFLD	79
6.2.3 Bearing GG genotype from PNPLA3 rs738409 confers susceptibility to NASH development	80
6.2.4 Carrying A-allele from FGF21 rs838133 confers susceptibility to significant fibrosis	83
6.2.5 Identification of target microRNAs: miR-200b-3p and miR-224-5p.....	86
6.2.6 Both liver miR-200b and miR-224 are induced in NASH, steatosis and ballooning.	86
6.2.7 Plasma miR-200b and miR-224 are induced in NASH but not in significant fibrosis, steatosis or ballooning.....	88
7. DISCUSSION	91
8. CONCLUSIONS	104
9- REFERENCES	106

SUMMARY

Non-alcoholic fatty liver disease (NAFLD) has become one of the top concerns for the practising hepato-gastroenterologist due to the obesity epidemic and its potential to progress to an advanced liver disease that significantly impacts on overall and liver-related mortality. Due to the rapidly advancing epidemics of obesity and diabetes, a large segment of the population is at risk for NAFLD. Particularly worrisome is the emergence of NAFLD or non-alcoholic steatohepatitis (NASH) with a significant fibrotic disease in developing countries, even in patients of normal or underweight.

A critical issue in patients with NAFLD is the differentiation of NASH from simple steatosis (SS). It is then of particular importance to identify NASH patients as they are at greatest risk of developing cardiovascular diseases and complications such as cirrhosis, liver failure or hepatocellular carcinoma.

There is a need, in NAFLD management, to develop non-invasive methods to detect NASH and to predict advanced fibrosis stages. Therefore, we evaluated the following items:

(i) A tool-based on optical analysis of liver magnetic resonance images as biomarkers for NASH and fibrosis detection by investigating patients with biopsy-proven NAFLD who underwent magnetic resonance protocols using 1.5T General Electric or Philips devices. Two imaging biomarkers (NASHMRI and FibroMRI) were developed, standardized and validated using the area under the receiver operating characteristic curve (AUROC) analysis. The results indicated NASHMRI diagnostic accuracy for steatohepatitis detection was 0.83 (95%CI: 0.73-0.93), and FibroMRI diagnostic accuracy for significant fibrosis determination was 0.85 (95%CI: 0.77-0.94). These findings were independent of the magnetic resonance system used. We conclude that the optical analysis of magnetic resonance images has high potential to define non-invasive imaging biomarkers for the detection of steatohepatitis (NASHMRI) and the prediction of significant fibrosis (FibroMRI).

(ii) Genetic and epigenetic biomarkers, such as human patatin-like phospholipase domain containing 3 (PNPLA3), transmembrane 6 superfamily 2 (TM6SF2) and fibroblast growth factor 21 (FGF21) variants as well as a panel of most abundant liver microRNAs. After univariate and multivariate analysis, we confirmed that GG genotype of PNPLA3 exerted a clear role in NASH development, and we identified the impact of a novel risk variant located in FGF21 gene in significant fibrosis stages. Besides, we found overexpression of FGF21 levels in both liver and serum, directly related to NASH condition. Finally, two microRNAs (miR-200b-3p and miR-224-5p) were screened and validated in human liver tissue and plasma of biopsy proven NAFLD patients, and were found raised in NASH, conferring them potential as non-invasive biomarkers.

BACKGROUND

1.1 Non-alcoholic fatty liver disease concept, epidemiology, comorbidities, complications, and pathophysiology

Non-alcoholic fatty liver disease (NAFLD) is one of the most common causes of hepatic disease worldwide, and its rates are growing together with metabolic syndrome. It has been considered not just the hepatic manifestation of metabolic syndrome in the liver but also a key factor in the development of complications related to metabolic syndrome (1).

This disorder is usually classified into two different phenotypes, simple steatosis (SS) and non-alcoholic steatohepatitis (NASH), accompanied with various fibrosis stages. This entity comprises a broad spectrum of lesions ranging from simple steatosis to steatohepatitis (defined by inflammation and ballooning). These patients could show fibrosis progression to cirrhosis, being at risk of potentially life-threatening liver-related complications, such as hepatocellular carcinoma, cirrhosis decompensation or requiring orthotropic liver transplantation (2). Cirrhosis describes the fibrosis or scarring that occurs as part of a wound healing response to non-alcoholic steatohepatitis, which is commonly called NASH (figures 1 and 2).

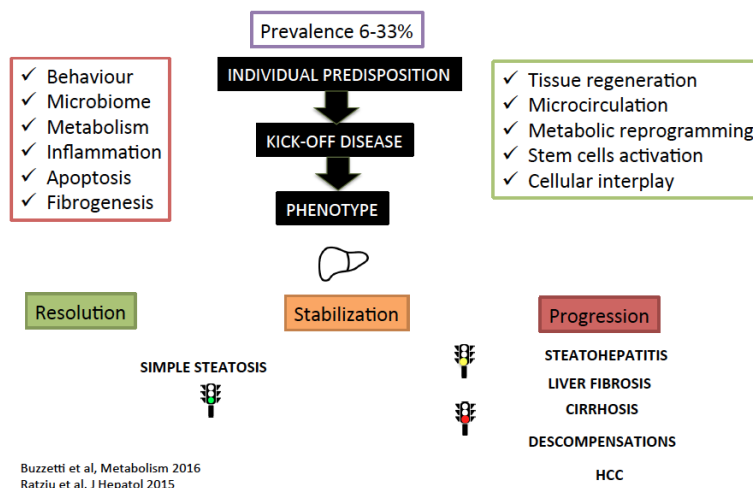


Figure 1. Non-alcoholic fatty liver disease spectrum.

In fact, the increased incidence of NASH and fibrosis has been found directly related to a raised mortality and morbidity. Besides, NAFLD is becoming the leading cause of liver transplantation for both end-stage liver disease and hepatocellular carcinoma in the United States (3). Hence, if the current rates of obesity and diabetes continue for another two decades, the prevalence of NAFLD in the world is expected to increase by 50% in 2030, leading to an epidemic of NAFLD.

The dogma supporting that NASH patients but not simple steatosis were at risk of liver disease progression seems to be controversial (4, 5). Patients suffering from simple steatosis trend to progress to NASH and to develop fibrosis in paired liver biopsies during short-term follow-up between 3 to 6 years. Together to the risk of fibrosis progression sample error should be kept in mind. Further, fibrosis staging in NAFLD showed a good concordance between pathologists but fibrosis distribution in the liver is heterogeneous, and it could be found different stages of fibrosis in the same liver, in the same patient. Thus, it is mandatory to segregate patients according to NASH presence but also close monitoring it using non-invasive methods to classify patients according to the risk of progression. Metabolic syndrome, hyperinsulinemic state, and diabetes seem to belong to the most dangerous phenotype implicated in disease progression (6). However, hyperlipidaemia and obesity seem to be more heterogenic influencing on disease progression. Interestingly, men are at higher risk of having severe fibrosis compared to women, at least before menopause.

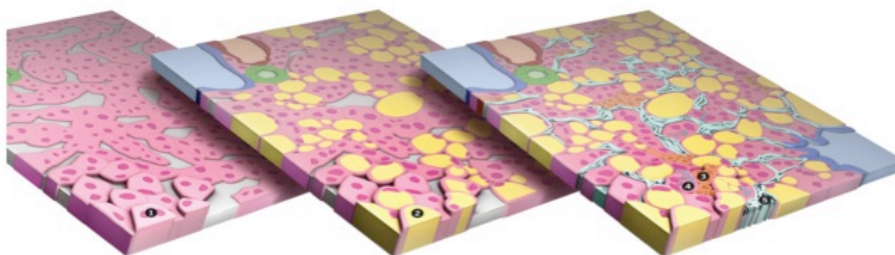


Figure 2. A healthy liver (1) can progress to fat accumulation (2) and then to NASH, which features inflammation (3), cell swelling (4), and sometimes scarring (5) (7).

Patients with NASH-cirrhosis are at risk to develop complications and outcomes such as hepatocellular carcinoma or cirrhosis decompensation. In comparison with hepatitis C-related (HCV) cirrhosis, NASH-cirrhosis showed a lower rate of cirrhosis decompensation mainly in ascites development. Hepatocellular carcinoma rate has been estimated in 0.67% cases per year in NASH-cirrhosis in comparison with 1.7% per year in HCV-cirrhosis (8). Patients suffering from NASH-cirrhosis showed higher mortality due to cardiovascular disease. Changes in hepatic blood flow in NAFLD patients occurred during the earliest stages of fibrosis due to the outflow block in the sinusoidal area, as well as increased splenic stiffness (9). Moreover, according to the SRTR (Scientific Registry of Transplant Recipients) in United States, NASH-related cirrhosis is currently the third most common indication for liver transplantation overtaken by hepatitis C virus and alcoholic cirrhosis (10).

NAFLD is closely associated with features of metabolic syndrome, such as abdominal obesity, atherogenic dyslipidaemia, hypertension, insulin resistance and impaired glucose tolerance. The majority of patients showing NAFLD has, at least, one of these characteristics and up to one-third can present the whole syndrome (11). Thus, this entity shares multiple potential risk factors with cardiovascular disease (12).

Interestingly, cardiovascular disease is the main cause of complications in NAFLD. In fact, several meta-analyses have reported this association (13). By contrast, chronic liver disease is the responsible for most of morbidity and mortality in NASH stage (14). A routine assessment of the cardiovascular risk seems to be adequate in patients with NAFLD. To reach this aim, several non-invasive methods have been proposed. Firstly, carotid disease is an independent entity that can predict stroke (15) and cardiovascular events (16). To evaluate

carotid disease, we can measure carotid intima-media thickness and the presence of carotid plaques by ultrasound. A thickness > 9 millimetres (mm) is considered pathological. This test seems to be the most used in NAFLD patients. Secondly, the number of coronary artery calcifications is directly related to cardiovascular events. This evaluation is performed by computerized tomography (17). Thirdly, left ventricular hypertrophy has been reported to increase the number of cardiovascular-related events and can be easily diagnosed by electrocardiogram and echocardiogram (18). Fourthly, there are tests whose aim is to detect blood vessel abnormal function. In particular, ankle-brachial pressure index identifies the presence of peripheral arterial disease and flow-mediated dilation detects endothelial dysfunction (19). Lastly, biomarkers (i.e. C-Reactive Protein (CRP) or Tumour Necrosis Factor alpha (TNF- α)) could be a good option to evaluate the cardiovascular risk although they need to be more extensively validated.

Recent data from both human and animal studies support the concept that the hepatocellular injury that characterizes NASH is mainly driven by the overload of primary metabolic substrates, such as glucose, fructose and fatty acids in the liver, leading to a diversion of fatty acids into different pathways that could promote different cellular injuries and a dysfunctional response to that damage. Anyway, various aspects of those pathways leading to both NASH and liver fibrosis vary among patients, as this is considered a multifactorial entity (20, 21). Pathogenesis of the illness is unclear with the most widely supported theory implicating insulin resistance and impaired lipid metabolism that leads to fat accumulation in the liver, as the fundamental mechanisms. Some researchers also support that a second hit, or additional oxidative injury, is required to manifest the necroinflammatory component of steatohepatitis; this results from a combination of mitochondrial dysfunction, oxidative stress, lipid peroxidation, hormonal abnormalities and cellular toxicity from free fatty acids (FFAs) (22). Mitochondrial dysfunction is also crucial in the pathogenesis of

NAFLD leading to overproduction of reactive oxygen species (ROS) that promote hepatocyte injury. Oxidative stress triggers cell membrane peroxidation, cell degeneration and apoptosis, and the expression of pro-inflammatory and pro-fibrogenic cytokines leading to progressive liver damage. NAFLD/NASH is considered as a chronic inflammatory disease, while cytokines have been linked to the development and prognosis (figure 3).

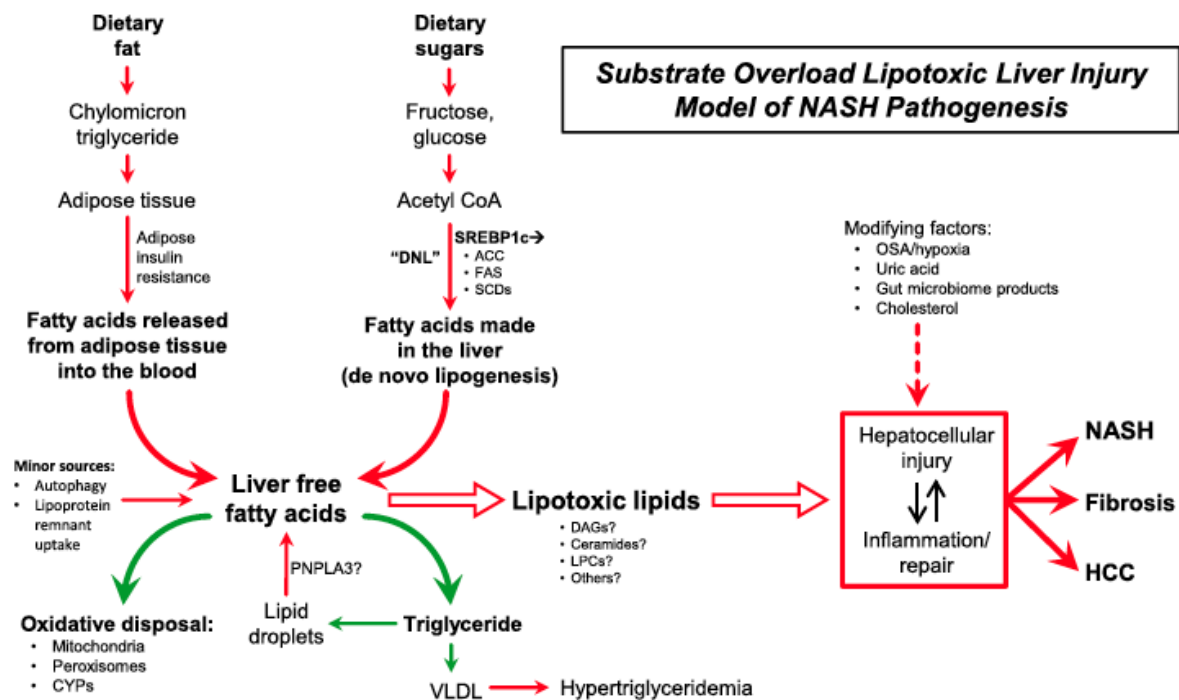


Figure 3. NASH pathogenesis model.

1.2 Management and care of patients with NAFLD

Management of non-alcoholic fatty liver disease (NAFLD) in clinical practice is a current and permanent challenge. The main aim is to segregate patients according to risk for disease progression keeping in mind both endpoints, liver and cardiovascular diseases. Patients referred for NAFLD study usually show hyperechogenicity of the liver in ultrasonography or increased transaminases together with features of metabolic syndrome. In non-hyperechogenic liver, suspicion should be delayed to demonstrate negative etiologic study.

Monitoring of these patients is mainly based on the histological findings and the associated diseases. There are three key areas to consider in handling NAFLD patients:

- a) Lifestyle modifications, including diet and exercise (23),
- b) Drugs targeting the components of metabolic syndrome and
- c) Managing of liver disease outcomes (24).

The optimal strategy remains unclear, but patients with NASH and fibrosis require more intensive lifestyle modifications and liver-directed pharmacotherapy, and if it fails, they need to be included in clinical trials.

Family history is an essential part of our routine medical evaluation and contains information on fatty liver, obesity, and diabetes. Indeed, several studies have shown familial clustering of NAFLD as well as its severity, especially in settings of coexisting insulin resistance (IR). In non-diabetic patients with NASH, a family history of diabetes could be found in more than 40%, and these patients showed increased risk of fibrosis progression. *Patient history* should include central obesity, type 2 diabetes, dyslipidaemia, and hypertension to recognize metabolic syndrome. Also, evidence of menopausal status, biliary gallstones, obstructive sleep apnoea syndrome, hyperuricemia, hypothyroidism, growth hormone deficiency, and polycystic ovary syndrome should be recorded.

Dietary habits using a diary recording adherence to Mediterranean diet and industrial fructose consumption; one protective and the other promoter of NASH risk. It is also mandatory to exclude excessive alcohol consumption by interview and analysis of biochemical variables including increased gamma-glutamyl transpeptidase (GGT) levels, aspartate/alanine transaminases (AST/ALT) ratio, mean corpuscular volume of erythrocytes, and carbohydrate-deficient transferrin levels (25). The average alcohol consumed (in grams) per day should be recorded. Alcohol consumption thresholds to define non-alcoholic nature of the steatohepatitis include < 21 units of alcohol per week for men and 14 units of alcohol

per week for women over a 2-year time frame before evaluation. One unit of a standard drink is equivalent to a 12-ounce beer, 4-ounce glass of wine, or one-ounce shot of distilled liquor. The significant social and economic impact across Europe means that effective management strategies NAFLD are urgently needed.

1.3 Current diagnosis: liver biopsy assessment

The current gold standard method for the assessment of hepatic fibrosis and NASH relies on liver biopsy, although its confirmed limitations include bleeding, perforation, death, and a high cost. These drawbacks imply several obstacles for the viability of clinical trials. Monitoring the natural progression of NAFLD by histology could generate a disproportionate number of liver biopsies compared to the rate of patients who develop severe complications.

Histopathological criteria for NASH diagnosis have changed over time, wherein fibrosis presence is not required for the diagnosis. Pathological classifications utilised are Matteoni classification (26), Brunt classification (27), NAFLD Activity Score (NAS) (28) and, most recently, Steatosis Activity and Fibrosis (SAF) Score (29, 30) (tables 1 and 2)

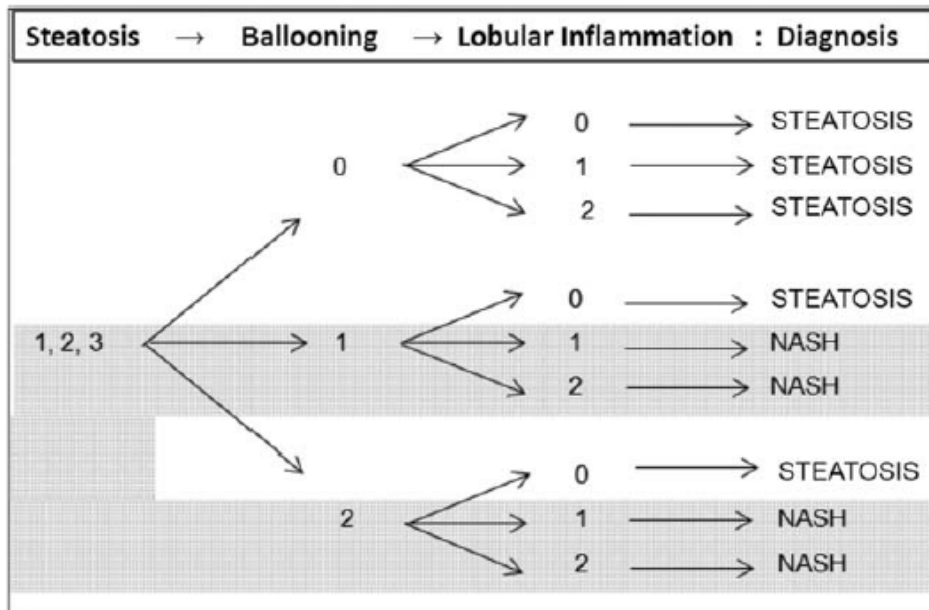
Moreover, it has been established hepatocellular ballooning as a key histological finding in NASH diagnosis, being a component of common NAFLD scores. Ballooned hepatocytes frequently contained Mallory-Denk bodies, and the main mechanisms implicated in ballooning degeneration are basically, rearrangement of intermediate filament cytoskeleton, accumulation of small-droplet fat in the cytoplasm and endoplasmic reticulum dilatation. All these mechanisms support a key role of ballooning on disease progression (31). In an elegant study by Ratziu et al., 51 patients underwent two liver biopsies that were scored separately. Steatosis, ballooning, inflammation and fibrosis seem not being equally distributed across the liver. In 21 out of 51 cases one stage difference in fibrosis was seen, and ballooning has been observed in just one liver biopsy in 9 out of 51. Thus, fibrosis stage variability was found around 40% and ballooning diagnosis around 20%. All these aspects

should be taken into account when analysing paired liver biopsies for disease progression or histological response (32).

Table 1. NASH Clinical Research Network (NASH-CRN) scoring systems definitions.

Item	Definition	Score/Code
Steatosis		
Grade	Low- to medium-power evaluation of parenchymal involvement by steatosis	
	<5%	0
	5%-33%	1
	>33%-66%	2
	>66%	3
Location	Predominant distribution pattern	
	Zone 3	0
	Zone 1	1
	Azonal	2
	Panacinar	3
Microvesicular steatosis*	Contiguous patches	
	Not present	0
	Present	1
Fibrosis		
Stage		
	None	0
	Perisinusoidal or periportal	1
	Mild, zone 3, perisinusoidal	1A
	Moderate, zone 3, perisinusoidal	1B
	Portal/periportal	1C
	Perisinusoidal and portal/periportal	2
	Bridging fibrosis	3
	Cirrhosis	4
Inflammation		
Lobular inflammation	Overall assessment of all inflammatory foci	
	No foci	0
	<2 foci per 200× field	1
	2-4 foci per 200× field	2
	>4 foci per 200× field	3
Microgranulomas	Small aggregates of macrophages	
	Absent	0
	Present	1
Large lipogranulomas	Usually in portal areas or adjacent to central veins	
	Absent	0
	Present	1
Portal inflammation	Assessed from low magnification	
	None to minimal	0
	Greater than minimal	1
Liver cell injury		
Ballooning*		
	None	0
	Few balloon cells	1
	Many cells/prominent ballooning	2
Acidophil bodies		
	None to rare†	0
	Many	1
Pigmented macrophages		
	None to rare†	0
	Many	1
Megamitochondria*		
	None to rare†	0
	Many	1
Other findings		
Mallory's hyaline	Visible on routine stains	
	None to rare†	0
	Many	1
Glycogenated nuclei	Contiguous patches	
	None to rare†	0
	Many	1

Table 2. SAF Score diagnostic algorithm for NASH.



1.4 Non-invasive diagnosis of NAFLD

Due to this increasing burden, there is an urgent need for reliable and accurate non-invasive methods to stage the disease, as well as identification an outburst of potential innovative therapeutic targets to inhibit the progression and associated risks of this disease. Among the top diagnostic concerns are the detection of NASH and liver fibrosis, as they have both been proven to increase the risk of mortality related to both liver and cardiovascular diseases (33, 34). Early detection of fibrosis and cirrhosis is essential due to the complications derived from these conditions, such as hepatic encephalopathy or gastro-oesophageal varices. Therefore, an urgent demand for reliable and accurate non-invasive approaches is emerging.

The epidemic of NAFLD/NASH is a clear threat to public health and healthcare systems. There are gender and ethnic differences, the latter possibly attributed to different lifestyle and dietary patterns, insulin resistance, adiposity distribution and genetic variations. To date, various non-invasive biomarkers have been identified; however, they lack accuracy,

especially in certain sub-populations, and usually, need external validation before being applied in clinical practice.

Further, NAFLD is a multifactorial disease affected by both environmental and genetic factors, and its precise pathogenesis is still not fully understood. According to the National Institutes of Health (NIH) definition-working group, the description of a biomarker (35) is a characteristic that is objectively measured and evaluated as an indication of normal biologic processes, pathogenic processes or pharmacological responses to a therapeutic intervention. To our understanding, the ideal test should be economical, widely accepted, bias-free, and reflective of the biological phenomenon studied and validated through sensitivity, specificity, and predictive capacity (figure 4).

Screening biomarkers to detect susceptibility, together with prognostic biomarkers for disease progression, and finally, response biomarkers to therapy could improve the management of NAFLD. The successful search of a new biomarker depends on strengthen of the definition of the end-point, the more accurate end-point, the better biomarker. The main features of a biomarker include from A to F: Acceptability; Bias of process selection of the candidate; Cost of tests; Diagnostic accuracy; Errors measurement and Feasibility. They should demonstrate ability to predict baseline presence of NASH and fibrosis stage together with the possibility of detecting NASH resolution and fibrosis regression after therapeutic intervention. The most important aspects included in the validation process comprise:

- (i) Content validity, the biomarker should reflect the biological process studied,
- (ii) Construct validity, in the disease manifestation and
- (iii) Criterion validity, the biomarker correlates with the particular disease and should be measured by sensitivity, specificity, and predictive power.

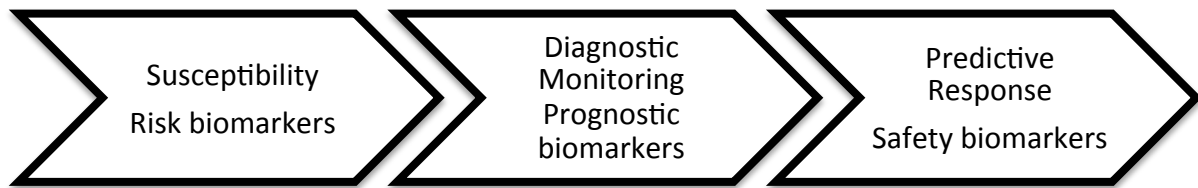


Figure 4. Cluster of biomarkers according to FDA/NIH.

Following the EASL guidelines, in order to reduce the number of liver biopsies, non-invasive markers should aim to:

- i) In primary care settings, identify the risk of NAFLD among individuals with increased metabolic risk,
- ii) In secondary and tertiary care settings, identify those with worse prognosis, e.g. severe NASH,
- iii) Monitor disease progression and
- iv) Predict response to therapeutic interventions (36).

This epigraph will be divided into the three primary categories of non-invasive assessment of NAFLD: imaging, biochemical and genetic biomarkers (figure 5).

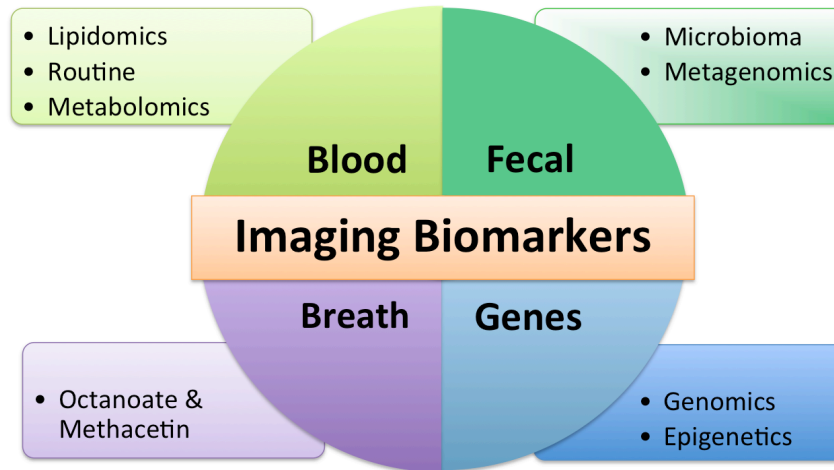


Figure 5. Non-invasive approaches spectrum for NAFLD diagnosis.

1.4.1. Imaging biomarkers

Significant improvements have been made in the field of imaging techniques, placing them as highly accurate diagnostic tools, with strong potential for NAFLD detection.

Abdominal ultrasound (US) is used as a routine first-line screening, diagnosis, and follow-up of NAFLD patients. Among the main features of NAFLD is hyperechogenicity, increased liver size, vascular blunting or attenuation of the ultrasound wave (37). However, this method is operator-dependent, and when fat infiltration is less than 30%, US is unable to detect steatosis, and the sensitivity of this technique ranges between 60-84%, and the specificity is among 84-95%, which increases in parallel of the severity of steatosis (38).

Computed tomography (CT) could be used to diagnose steatosis by comparing spleen and liver attenuation values but is not sensitive stratifying and detecting fibrosis stage. CT is also unable to detect steatosis when there is less than 30% of fat in the liver (39). Additionally, it exposes patients to radiation, and therefore its use for NAFLD detection is less common.

Magnetic resonance imaging (MRI) techniques can quantify both fat and liver fibrosis. Hepatic steatosis is commonly measured by evaluating the proton density fat fraction

(PDF) and has been validated across various sub-populations, demonstrating that several confounding factors, such as age, sex, body mass index and disease components have no substantial impact on its diagnostic accuracy. This technique also offers an excellent reliability and reproducibility, also responding to changes over time (40). However, this approach still has several restrictions, such as the small portion of the liver analysed, the expertise needed to acquire and quantify the images and its high running cost. Regarding fat evaluation, multi-echo MRI fat fraction has also been proposed as an attractive tool to determine the hepatic lipid concentration in NAFLD obese patients (a specific subpopulation especially hard to diagnose) (41). Other novel MRI techniques have been developed to quantify the main features of this disease.

Retrospective and prospective studies reported that magnetic resonance elastography (MRE) has shown a high diagnostic accuracy in staging fibrosis in NAFLD patients, specially diagnosing advanced fibrosis stages, such as F3-F4, independently of BMI and inflammatory status (42), but not for NASH. Furthermore, in a recent study carried out in more than 100 liver biopsy-proven NAFLD patients, MRE was found to be more accurate than transient elastography identification of liver fibrosis, from stage 1 of the disease (43). Lastly, liver stiffness measured by MRE has been shown to have high accuracy as defined by the area under the receiver operating characteristic curve (AUROC = 0.93) for discriminating patients with NASH from those with SS, with 94% sensitivity and 73% specificity (44).

Magnetic resonance spectroscopy (MRS) detects small quantities of fat as it identifies spectral peaks at resonance frequencies precise to the protons in triglycerides. Recent studies on cellular based-metabolism biomarkers in high-fat diet rats for non-invasive steatosis assessment (45), by hyperpolarized ¹³C magnetic resonance spectroscopy, suggested the potential use of MRS for steatosis diagnosis. The main limitation of this study was the small

number of animals included, which was six rats per group, and the fact that metabolic changes were measured only from a single localized voxel.

Liver stiffness measurement has been widely utilized in chronic viral hepatitis and has been extrapolated to NAFLD. Transient elastography (TE), brand named FibroScan, has been used to measure liver stiffness in NAFLD patients, and seems to be accurate enough to predict the stage of fibrosis, showing an AUROC higher than 0.83 (46). Nevertheless, these results can be influenced by obesity and the degree of steatosis, leading to potentially false-positive results (47). Body mass index higher than 28 kg/m² was related to higher failures rate (4.5%). Cut-off values defining fibrotic stages in NAFLD measured by FibroScan® varied among the reports (4, 48, 49) and failure rate range from 5% to 19% (50). The new XL probe achieves higher successful rates than M probe, although surprisingly, cut-off points have been suggested to be lower than those for the M probe (51).

Recently, a new tool has emerged, provided by the same device, which uses similar probes to TE, called controlled attenuation parameter (CAP), capable of detecting hepatic steatosis. A recent study designed to evaluate whether the liver stiffness could be influenced by CAP measurements, suggested that CAP values should always be considered to avoid overestimation of liver fibrosis when assessed by TE (52). However, a recent cross-sectional study has demonstrated that MRE and PDFF showed higher diagnostic accuracy in liver fibrosis and steatosis detection in comparison to TE and CAP methods (53, 54).

Finally, few studies have evaluated the diagnostic accuracy of acoustic radiation force impulse (ARFI) in NAFLD patients, trying to differentiate between fibrosis stages (55-57) and incorporating patients with morbid obesity (58). The main limitation of this method is the narrow ranges for stratification of fibrosis that can difficult an adequate patient management in clinical practice.

1.4.2. Serum biomarkers

A serum biomarker is a measurable substance that can be used as an indicator of a biological condition. Different algorithms of serum biomarkers for fibrosis staging or NASH detection include combinations of direct or indirect markers that have been proposed to exclude severe disease and risk stratification and to provide valuable prognostic information of hepatic and non-liver related comorbidities. Further, several commercial marker panels have been evaluated for their ability to distinguish among disease stages, although these panels are still limited by their high cost.

Cytokeratin-18 (CK-18) is a major intermediate filament protein found in the liver, which is generated during cell death (M65) or apoptosis (M30). Its secretion into the serum makes it a measurable condition. Raised levels of CK-18 are able to distinguish between SS and NASH, but currently, the AUROC ranges between 0.71 and 0.93 (59, 60) and are associated with fibrosis and inflammation (61).

Fibroblast growth factor 21 (FGF21) is a member of the fibroblast growth factor family that regulates lipid metabolism and reduces hepatic lipid accumulation in an insulin-independent manner (62). FGF21 is secreted as an endocrine factor to coordinate the adaptive response to starvation or fasting, or as an autocrine factor induced in adipose tissue during the fed state to regulate adipocyte function (63). FGF21 arbitrates the crosstalk between different metabolic organs to regulate glucose and lipid metabolism through pleiotropic actions in these tissues and the brain. The liver regulates carbohydrate production through hepatic FGF21 generation, suppressing single sugars consumption but not complex carbohydrates, proteins or lipids (64). FGF21 has been proposed as a protective factor in metabolic disorders in various animal models. Administration of recombinant Fgf21 in diabetic rhesus monkeys has revealed potent *in vivo* benefits on glucose and lipid metabolism, insulin sensitivity and body weight without effects on cell proliferation and tumorigenesis (65, 66). Several human

studies have reported that circulating FGF21 levels are increased in metabolic syndrome (67), obesity (68), type 2 diabetes mellitus (69), hypertriglyceridemia (70) and NAFLD (71, 72). Since FGF21 is synthesized in the hepatocyte, it is rational to consider that pathological liver alterations could modify its expression. Hereby, FGF21 messenger RNA (mRNA) was found increased in NAFLD human liver, but not in NASH (73). This fact could be related to FGF21 resistance (74). Moreover, treatment with LY2405319, a recombinant variant of FGF21, causes significant dyslipidaemia amelioration in obese humans with type 2 diabetes mellitus (75). Lately, in a two-stage genome-wide meta-analysis designed to identify common genetic variants associated with total energy intake from different sources, a single-nucleotide-polymorphism (SNP) located in FGF21 gene (rs838133) was related to decrease the protein intake and increase the carbohydrate ingestion (76).

Other markers of NAFLD hepatocyte inflammation include adiponectin, TNF- α , leptin and resistin, associated with obesity-related diseases, such as NAFLD. Various serum markers have shown a moderate diagnostic accuracy with an AUROC higher than 0.8.

Several panels of routinely available serum biomarkers can confirm, or rule out, significant fibrosis in NAFLD patients. NAFLD Fibrosis Score (NFS) (77) is a blood test specifically designed to evaluate liver fibrosis in NAFLD, with validated diagnostic accuracy (78), but according to the two thresholds, this marker still has a grey zone (> -1.455 to < 0.675), that could reach from 25% to 56% of the cases, thereby a liver biopsy is needed. Diagnosis accuracy is high when results are over or under cut-offs defining no advanced fibrosis (NFS < -1.455) and advanced fibrosis (NFS > 0.675) (positive predictive value (PPV) 82%-90% and negative predictive value (NPV) 88%-93%). However, high NFS levels have been associated with raised risk of systemic events, especially cardiovascular complications (79).

Further, FibroMeter® development was aimed to find a specifically designed NAFLD test for significant hepatic fibrosis, but is less sensitive than NFS for advanced fibrosis discrimination (80).

AST to Platelet Ratio Index (APRI index) (81) and Forns score (82) were initially developed in patients with chronic hepatitis C but were both represented with a moderate diagnostic accuracy when applied in NAFLD (83). On the other hand, FIB-4 test had the same initial purpose, but its diagnostic accuracy is similar to NFS in advanced fibrosis determination (84). They are routinely used in chronic hepatitis to exclude advanced disease because are cheap and easy to perform they have been used in clinical practice. Considering the parameters the availability of the lab parameters could be an election method to rule out advanced fibrosis, but it was found unable to distinguish among SS and NASH. Further, these methods were developed in chronic hepatitis and thresholds could not be transferred to NAFLD without previous estimation, validation and standardization process. Sidney's index (85) showed a high potential to exclude advanced fibrosis in chronic hepatitis C, incorporating insulin resistance to improve diagnostic accuracy of different biochemical methods. BARD score (86) also excludes patients with advanced fibrosis, especially in non-diabetic populations, and more recently, it has been found useful for excluding liver fibrosis in bariatric populations (87).

Several serum biomarkers have been integrated into mathematical models to generate predictive scores. Fibromax® constitutes a quantitative panel of serum biomarkers as an association of three tests (Fibrotest®, Steatotest®, and NashTest®) that offers information about fibrosis, steatosis, and necroinflammatory activity or NASH (88). It has been validated in chronic hepatitis C (89) and steatosis (90). It has been recently reported that FibroTest® and Steatotest® have prognostic values for predicting survival in patients with metabolic disorders (91). This algorithm combines various clinical and biochemical parameters to detect

all the spectra of NAFLD conditions, including steatosis, NASH, inflammation, and fibrosis. Although this became very popular and reached important diagnostic accuracy, higher than 0.83 in every condition (92), it is not easy to perform in clinic, as some of the variables are not available in routine lab assays.

Finally, OWLiver® (93) analyses the metabolic profile of NAFLD patients by evaluating 540 serum metabolites using ultraperformance liquid chromatography coupled to mass spectrometry (UPLC-MS) to discriminate among SS and NASH. Although the AUROC supports a high diagnostic accuracy for NASH according to body mass index (0.85), the main limitations are the scarce availability of this technique requiring to be processed in a central lab and the inability to distinguish fibrosis. Among all these tests, only NFS and FIB-4 have been externally validated more than once in different populations (94).

1.4.3 Genetic and epigenetic biomarkers

In the majority of patients, NAFLD is a multicomponent disease rooted in metabolic syndrome features. Due to the substantial variation in terms of disease severity and mortality risks, beyond environmental factors, once the complete genome was fully published, a major part of the research has focused on genetic implications in each stage of NAFLD pathophysiology.

Genome-wide associations studies (GWAS) have considerably increased the knowledge of identifying novel players associated with NAFLD pathogenesis, constituting a powerful tool. Among these, single nucleotide polymorphisms (SNPs) have received growing attention, revealing new pathogenic loci and generating new biological hypotheses. They have been associated with SS and oxidative stress, inflammation, liver fibrosis and lastly, hepatocellular carcinoma. Although liver biopsy is still considered the gold standard for the evaluation of liver disease, it is still limited by variability and sampling error. Therefore, the

incorporation of an unalterable genetic marker for liver fibrosis or NASH to a predictive algorithm could provide an increased diagnostic accuracy.

Epidemiological, familiar and twin studies have provided enough shreds of evidence for NAFLD spectra heritability. Different familial clustering studies have demonstrated the heritable component of NAFLD. One study conducted on eight kindred showed that at least 50% of members were affected by various patterns of relatives and conditions (95).

To this regard, twin studies offer valuable information. In a recent study performed in 60 pairs of twins, hepatic steatosis and liver fibrosis were found strongly correlated in monozygotic twins but not in dizygotic twins, supporting the hypothesis that they are heritable traits (96).

In 2008, Romeo *et al* discovered a variant in a GWAS performed in a population-based study where hepatic liver content was measured by magnetic spectroscopy (97). This SNP was located in the PNPLA3 gene on chromosome twenty-two, which codes for a protein with lipase activity towards triglycerides in hepatocytes. This isoleucine to methionine substitution results in a loss of function leading to the accumulation of triglyceride in hepatocytes, which in turn effects the development and progression of NAFLD. Further replication studies have shown robust associations between PNPLA3 and steatosis, fibrosis, cirrhosis, and hepatocellular carcinoma (98), even conferring susceptibility to lifestyle modifications (99).

Subsequently, GWAS revealed other common SNPs associated with fat accumulation in liver. Those SNPs could modify or not the aminoacidic sequence, are stably inherited and confers susceptibility to disease development or pharmacological or non-pharmacological treatment response. More recently a nonsynonymous single nucleotide polymorphism (SNP) in transmembrane 6 superfamily member 2 (TM6SF2), located on chromosome 19, was associated with hepatic triglyceride content (HTGC) as measured by proton magnetic

resonance spectroscopy ($^1\text{H-MRS}$) (100). This missense variant (rs58542926 C>T) replaces glutamate with lysine, and was found associated with liver fat content, reduced plasma lipid levels and increased levels of circulating liver enzymes. Besides, it was shown to be related to advanced fibrosis and cirrhosis (101) and its protein is required to mobilize lipids for VLDL assembly. Further, carriers of this risk variant appear to be protected against cardiovascular disease, but are more susceptible to develop NASH (102). This effect was independent of PNPLA3 rs738409 effect, obesity and insulin resistance or alcohol intake.

The identification of novel genetic risk variants and the introduction of predictive models could be useful tools for the clinical management and stratification of patients at risk. Next-generation approaches could soon develop more precise genetic biomarkers, which should be cost-effective technologies applicable to clinical practice (figure 6).

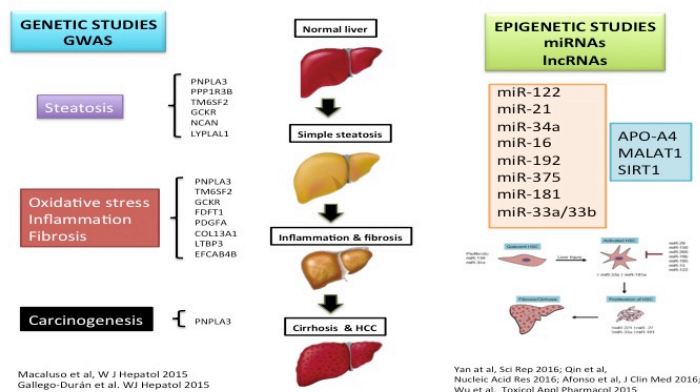


Figure 6. Most relevant genetic and epigenetic studies carried out for different NAFLD features.

Hence, there is a need for novel molecular markers that could help in early and moderate disease stages. Knowledge of epigenetics and heritable events not caused by changes in DNA sequence have contributed to the development of broad spectra of diseases has been a revolution in the past few years. More recently, evidence is accumulating to reveal

the fundamental role of epigenetics in NAFLD pathogenesis and NASH genesis (103). Among the main epigenetic mechanisms, microRNAs have received growing attention.

MicroRNAs or miRNAs are highly conserved, naturally occurring, single-stranded, non-coding RNA molecules that are less than 25 nucleotides long. They modulate several biological situations by regulating gene expression at post-transcriptional levels. Additionally, they are usually deregulated under pathological conditions, around 30% of mRNA expression, and exert their function by pairing with complementary sequences of target mRNA. Since they are present in many biofluids, they offer a great potential as non-invasive biomarkers. Circulating miRNAs are highly stable in serum or plasma samples, free or packaged for protection against RNase activity. Latest advances in molecular biology have enhanced our knowledge about genotype-phenotype relationships, and several miRNAs have been used as biomarkers to detect NAFLD injuries. However, the main difficulties remain in standardization procedures and high cost, which is necessary before their translation into clinic (table 3).

Table 3. Summary of non-invasive methods for main NAFLD features

STEATOSIS	NASH	FIBROSIS
CT	CK-18	NFS
CAP	FGF21	FibroTest®
MRS	OWL-Liver®	FibroMeter®
SteatoTest®	NashTest®	Transient elastography
PDFF-MRI	Genetics	Forns, APRI, FIB-4
¹³ C-MRS	Epigenetics	MRE
		ARFI

HYPOTHESIS

NAFLD encompasses two distinct entities, a benign simple steatosis and its progressive form, NASH, which can lead to severe outcomes. Steatohepatitis and advanced fibrosis have been associated with an increased mortality rate between 5 and 10 times respectively. Indeed, NASH can evolve towards cirrhosis and hepatocellular carcinoma. Nevertheless, it is possible to stop or slow disease progression by life-style intervention and pharmacological treatment. Currently, new insights into its progression, particularly concerning identifying the initiating mechanisms and patients at risk, as well as developing innovative diagnostic methods adapted for large scale screening evaluation. In order to define prognosis and appropriate therapeutic management, a critical issue is the differentiation of NASH from simple steatosis that remains a major clinical challenge.

Based upon the knowledge that accurate diagnosis, effective treatment and operative tools to monitor disease response are the three pillars essential in support of medical practice; thus, the development of an accurate, reliable, non-invasive and cost-effective tool is mandatory.

Thus, considering that both liver fibrosis and NASH generate several morphological changes in tissue structures that could be determined by optical analysis of magnetic resonance images, the relationship between this analysis and tissue alteration due to the disease could be patterned, to diagnose the disease.

Genetic markers are heritated stably and pose a substantial predictive capacity not influenced by external agents. Finally, taking into account circulating microRNAs are highly stable in serum or plasma samples, and currently there is a wide range of miRNAs profile technologies based on sequence specificity, both small non-codifying molecules and genetic variants could constitute powerful non-invasive diagnostic tools.

AIMS

In the current study, the main aim was to develop, standardise and validate imaging biomarkers defined by optical processing methods applied to conventional non-enhanced contrast magnetic resonance images to predict, using non-invasive tools, steatohepatitis and fibrosis stages in NAFLD patients.

The secondary objective was to identify, select and compare those emergent imaging biomarkers with currently available biochemical markers that will be transformative for the clinical management of patients.

Finally, the last aim was to identify novel genetic and epigenetic biomarkers that could be used as non-invasive tools for NASH and significant liver fibrosis detection.

RATIONALE

This project was initially designed considering the background evidence, need for the study, epidemiology of the underlying disorder and the magnitude of expected benefits over currently available diagnostic options. Number, location and centers involved were decided at the beginning of the study; however, three more Centres were incorporated during last year and a half to increase sample size and validate this approach.

Qualification process development included proof of concept, proof of mechanism, biomarkers acquisition and analysis, proof of principle and proof of efficacy and effectiveness.

The main aim, discrimination of NASH and significant fibrosis, did not change over time. After the consecution of this objective, it was integrated the supplementary non-invasive approaches to performing the comparative analysis.

MATERIAL AND METHODS

5.1 Patients, inclusion and exclusion criteria and ethical aspects of the research

Individuals were recruited from several Hepatology Units, and all patients provided informed consent for liver biopsy, MRI study and blood extraction (See annexed material).

They must fulfil, at least, two of the following three inclusion criteria: a) adults (≥ 18 years of age) who showed diffuse hyperechogenic liver on ultrasonography; b) impairment in biochemical liver profile, stated as sustained ALT or AST above ULN for at least 6 months; c) metabolic syndrome following ATPIII criteria (104). Exclusion criteria were: significant alcohol intake (>30 g/day in men and >20 g/day in women), recreational drugs abuse, pregnancy; parenteral nutrition, evidence of viral or autoimmune hepatitis, HIV, drug-induced fatty liver or other metabolic liver diseases (such as hemochromatosis or Wilson's disease), together with pregnancy and parenteral nutrition.

The study protocol conformed to the ethical guidelines of the 1975 Declaration of Helsinki, as revised in 1983. The Institutional Review Board Committee from each participating hospital approved the study protocol (Virgen Macarena-Virgen del Rocío University Hospitals, Valme University Hospital, Città della Salute e della Scienza di Torino Hospital, Marqués de Valdecilla University Hospital, Virgen de la Victoria University Hospital, Tajo University Hospital and Puerta de Hierro University Hospital) (see annexed material). Study procedures followed were in agreement with the ethical standards of the responsible committee on human experimentation, and were approved by the human research ethics committee from each Center.

All patients underwent a screening visit including medical history, physical examination, and laboratory tests. An electronic case report form (CRF) was employed to

warranty integrity and quality of data, and all aspects related to patients' privacy were considered. All data were coded, and the database was anonymized.

5. 2 Clinical, anthropometric and biochemical measurements

Patients underwent a complete medical history, physical examination, liver biopsy and imaging study. Clinical and laboratory data were collected at the same time of liver biopsy. Basic anthropometric data included body mass index (BMI), calculated as the weight in kilograms divided by the square of height in meters, and abdominal perimeter. Comorbidities included the presence of type 2 diabetes mellitus, arterial hypertension, and dyslipidaemia, and concomitant treatments at the time of biopsy were recorded.

An overnight (12h) fasting blood sample was taken at the same time of liver biopsy for routine biochemical analyses that were performed at the central laboratory of each University Hospital, to rule out occult diseases. Routine blood biochemistry and haematology analyses included the transaminases (ALT, AST), γ GT, alkaline phosphatase, total cholesterol, high-density lipoprotein cholesterol (HDL-c), low-density lipoprotein cholesterol (LDL-c), total bilirubin, albumin, triglycerides and viral serology for hepatitis B and C viruses. Serum insulin levels were measured by electrochemiluminescence immunoassay, using an Elecsys 1010/2010 autoanalyzer (Elecsys MODULAR ANALYTICS E170; Roche, Basel, Switzerland).

Samples were centrifuged 10 minutes at 3,500 revolutions per minute (rpm) right after obtained, alicuoted and immediately stored at -80°C until assayed. CK-18 was measured using a human enzyme-linked immunosorbent assay (ELISA) kit (Abnova, Walnut, CA, USA). Circulating *FGF21* levels were measured in 50uL using a human commercial ELISA assay (Biovendor, Karasek, Czech Republic) according to the manufacturer's instructions.

Inter-assay and intra-assay coefficients of variation were 3.3% and 2.0% respectively. Minimal detectable concentration was 7 pg/mL.

Finally, NAFLD Fibrosis Score (77) and Sydney Index (105) were calculated as previously reported and transient elastography was measured using FibroScan (Echosens, France) in fasting patients.

5.3 Histological staging and grading

Percutaneous liver biopsies were performed under local anaesthesia and ultrasound guidance. Liver specimens were obtained, after an overnight fast, by “tru-cut” needle (sample length/diameter = 20/1.2 mm) using a biopsy gun. At least one sample per patient was obtained. Lengths of liver specimens were recorded, as were the number of portal tracts. The sample was then assessed as being useful or not for histological diagnosis and fibrosis staging; samples of <10 mm length or <15 portal tracts were excluded. Biopsies were processed using standard procedures, formalin-fixed and paraffin-embedded and a fraction was immediately shock-frozen and stored at -80°C. Any adverse events from liver biopsy were reported.

A single pathologist, who was blinded with respect to provenance of the samples and unaware of clinical data, assessed the samples using haematoxylin-eosin, reticulin and Masson’s trichrome stains to determine the grading and staging assignments according to Kleiner et al (figure 7). This scoring system comprises four semi-quantitative features: steatosis, lobular inflammation, hepatocellular ballooning, and fibrosis. Steatohepatitis presence was not inferred from the NAS but, instead, was diagnosed taking into account patterns of histological distribution of lesions focusing on inflammatory activity and ballooning. Kleiner NAFLD Activity Score (NAS Score) and fibrosis stage were also

calculated. NAS Score provides an overall score that comprises the degree of steatosis (score 0-3), lobular inflammation (score 0-3) and hepatocyte ballooning (score 0-2).

Hepatic steatosis was quantified as the percentage of hepatocytes containing fat droplets, graded on a scale of 0-3 through subjective visual estimation of cells containing fat vacuoles. Steatosis grades were broadly categorised for severity: grade 0 or normal (up to 5% of hepatocytes affected); grade 1 or mild (5-33% of cells affected); grade 2 or moderate (33-66% showing steatosis); grade 3 or severe (>66% of hepatocytes showed fat storage).

Lobular inflammation was assessed as: grade 0 (non-inflammation); grade 1 (<2 foci/x200 field); grade 2 (2-4 foci/x200 field); grade 3 (>4 foci/x200 field). *Ballooning* was evaluated as: stage 0 (none); stage 1 (a few balloon cells); stage 2 (many cells or prominent ballooning). *Fibrosis staging* was based on a 5-level scale: F0=absence; F1=perisinusoidal or periportal; F2=perisinusoidal and portal/periportal; F3=bridging fibrosis; F4=cirrhosis.

A further 2-level scale of fibrosis was applied: mild (F0-F1) and significant (F2-F3-F4) fibrosis.

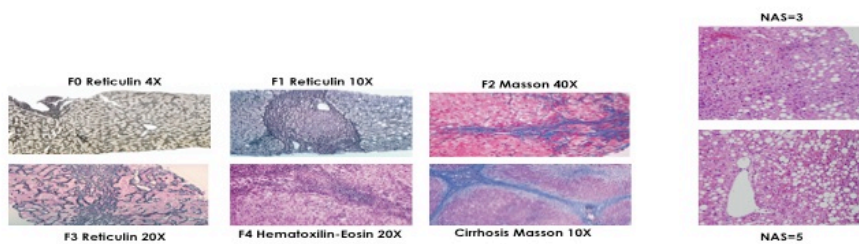


Figure 7. Histological findings in NAFLD patients.

5.4 Imaging biomarkers

5.4.1 Study design and patients

This was a cross-sectional and multi-centred study that included 126 well-characterised biopsy-proven NAFLD patients who were recruited between June 2009 and June 2013. Estimation cohort was enrolled from June 2009 to September 2010, and validation set from January 2010 to June 2013. Clinical data were collected at the time of liver biopsy using a particular case record form, together with blood samples for biochemical analyses.

The study sample was composed of all patients who fulfilled the inclusion criteria and were not disqualified by one or more of the exclusion criteria. Untreated and histologically confirmed NAFLD patients were recruited as part of the FLIP (Fatty Liver: Inhibition of Progression; www.flip-fp7.eu) project. The Fatty Liver Inhibition of Progression (FLIP) Consortium was formed in response to the FP7 call (figure 8). The aim of the FLIP project is to understand and prevent the progression of liver disease in NAFLD. The FLIP project is supported by the European Commission through the Seventh Framework Programme for Research and Development, and has been running since January 1st, 2010 (duration 36 months). Consortium Leader was Vlad Ratziu, and Prof. Romero-Gómez leded work package specifically dedicated to non-invasive and innovative diagnostic and prognostic biomarkers development.

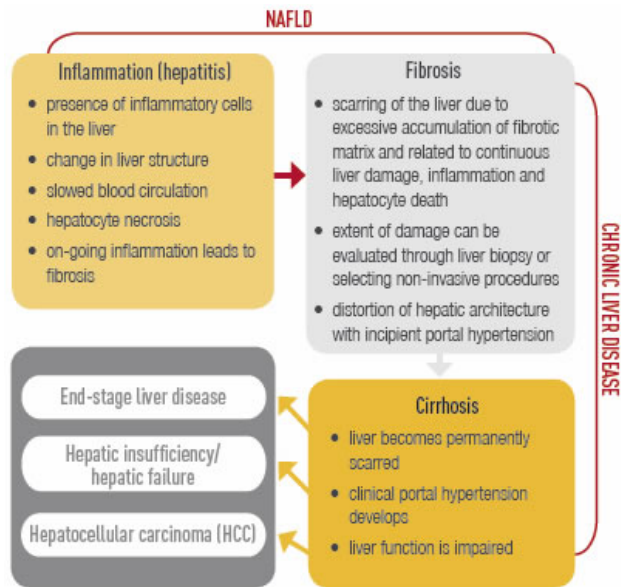


Figure 8. FLIP main outcomes and deliverables.

Patients enrolled in the study were classified according to sex, age, fibrosis stage and presence/absence of steatohepatitis.

5.4.2 Magnetic resonance image acquisition

MR studies were conducted at the six University Hospitals using General Electric (Milwaukee, CT, USA) or Philips (Best, NL.) 1.5-Tesla whole-body systems within a period of six months from liver biopsy. Patients were examined in the supine position using a standard torso coil centred over the liver. No contrast medium was used, and the patient was encouraged to individual breath-holding capacity by the technologist. MRIs were sent to the Referral Centre for processing in standard DICOM format. The images were processed and interpreted by two experienced engineers independently and, finally, a consensus was achieved. Both engineers were blinded to clinical and histopathological data. The entire liver was imaged, and 6 sections were selected covering the whole organ.

MR protocols for this study were performed in axial plane: SSFSE-T2 (Single Shot Fast Spin Echo T2-weighted), FAST-STIR (Fast Short inversion Time Inversion Recovery), inPHASE-outPHASE (in and out Phase) and DYNAMIC. DICOM files, the field of view

(FoV) and matrix sizes were configured specifically for each MR protocol; minimum and maximum window values were calculated so that each slice could be converted into a numerical matrix of pixels within the particular window range (table 4).

Table 4. Instructions to patients, preparation for imaging procedure, and imaging parameters recorded

INSTRUCTIONS	<ul style="list-style-type: none"> - Arms up if possible - Breath hold must be consistent - Supine position - Contrast: none
---------------------	--

Imaging parameters	Sequence name			
Imaging parameters	SSFSE-T2	FAST-STIR	In and out of PHASE	DYNAMIC
Scan plane	Axial	Axial	Axial	Axial
Imaging options	Breath hold	Breath hold	Breath hold	Breath hold
Time (sec)	29.76 \pm 10.05	340.98 \pm 104.10	38.10 \pm 6.66	35.44 \pm 90.33
FOV (mm)	450	400	410	375
Matrix size (px)	512x512	448x448	432x432	192x192

5.4.3 MR imaging processing to define NASHMRI and FibroMRI imaging biomarkers

5.4.3.1 Development and standardisation of imaging biomarkers

Thirty-nine patients were consecutively included in the estimation cohort; 20 (51%) had steatohepatitis, and 19 (49%) had significant fibrosis. The contour of the liver parenchyma is manually drawn in each slice. Each MR image is further divided according to a square grid that defines the set of samples (squares) to be processed. The spacing of the grid is chosen so that each sample square (from 10x10 pixels to 23x23 pixels, depending on image resolution and slice thickness) corresponds to an optimal volume of liver biopsy. Each sample is further

analysed to exclude those containing artefacts, such as vessels or biliary ducts. Also, those samples with >30% of its pixels outside the segmented area are discarded. Only those grid squares comprising liver parenchyma are analysed.

MR image features, segmentation algorithms, and implementation codes were developed in MATLAB (Matrix Laboratory, MathWorks, Natick, MA, USA) programming language. The software tool imports DICOM MR files and parses them, extracting all relevant information needed, including patient's clinical and demographic data from the MR protocol.

The image-processing algorithms comprise the following steps. First, the whole set of MR slices are presented to the user. The user, preferably those that contain the major liver section, must choose up to 6 consecutive slices (figure 9).

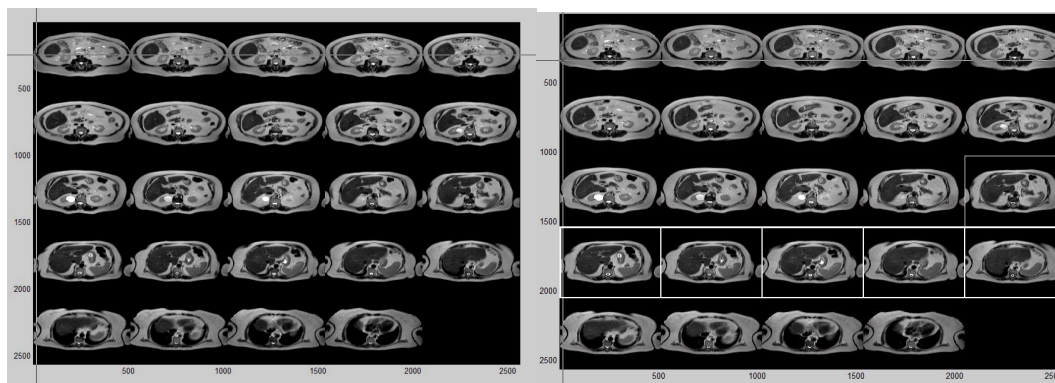


Figure 9. MRI acquisition and selection of six MR images containing liver

In each selected image, the user outlines the liver boundary (figure 10).

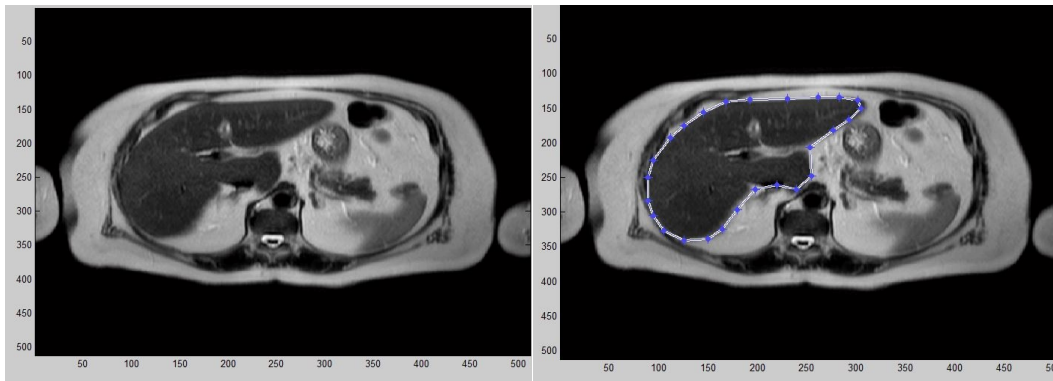


Figure 10. Presentation of selected slice and manual outlining of liver boundaries.

When the parenchyma is segmented, a square grid is automatically over-layered. Six slices and fifteen samples per slice are obtained, so around one hundred of valid samples per patient and protocol are extracted. To achieve a sample size (of each square) equivalent to a volume of 15 to 24 mm³ of tissue, the quantity of pixels of each sample is computed using the FoV, the number of rows and columns of the image matrix and the slice thickness. Therefore, the final amount of samples processed varies for different MR sequences, but this method increases diagnostic accuracy, due to liver biopsy analyses 1/50,000 of the whole liver, and using this approach this number is reduced to 1/25.

The software automatically discards those samples with >30% of the surface outside the segmentation line i.e. with a minimum of 70% pixels exhibiting liver parenchyma. The user must also reject samples that do not represent homogeneous liver tissue (i.e. those pixels containing vessels, ducts or other elements) (figure 11).

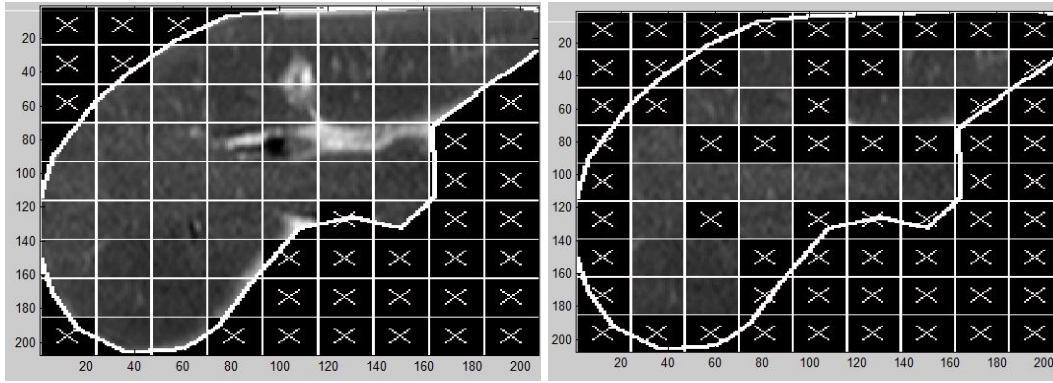


Figure 11. Segmentation, overlapping and valid sample selection process of the square grid.

A total of 84 different mathematical image parameters or "estimators" are computed from each sample. The nature of these parameters ranges from simple statistical descriptors such as mean and standard deviation to advanced image processing properties such as energy and entropy, geometrical properties like mean surface curvature, and spectral characteristics. All calculated parameters for each sample (patient and protocol), are related to clinical features (biochemical parameters and histological scores) of NASH and fibrosis using logistic regression to determine the optimal combination of protocols and parameters.

5.4.3.2 Validation of imaging biomarkers

The imaging biomarkers that were developed were validated in a cohort of 87 patients. No differences were observed concerning age, gender, steatosis degree, steatohepatitis or fibrosis distribution between the estimation and the validation cohorts. The average time consumed in MR studies was around 11 ± 3 minutes.

5.4.4 Comparison with biochemical biomarkers and transient elastography

NASH-MRI was compared with serum CK-18 levels. The FibroMRI was compared with Sydney Index, the NAFLD Fibrosis Score, and the transient elastography.

5.5 Genetic and epigenetic biomarkers

5.5.1 Patients and study design

This was a multicentre cross-sectional study including 225 biopsy-proven NAFLD patients showing different stages of the disease. Significant fibrosis was diagnosed in 22.2% (50/225) of the overall cohort, while NASH was present in 31.1% (52/167).

5.5.2 DNA isolation, quantification and single-nucleotide polymorphisms genotyping

Two-hundred-and-twenty-five biopsy-proven NAFLD patients were included (see table below). DNA was automatically isolated from 400 µL of whole blood by Magnapure® Compact equipment (Roche Diagnostics) following manufacturer's protocol. DNA quantification was performed by NanoDrop™ 2000® (Wilmington, USA) to avoid chemical interferences in the process. FGF21 rs838133, PNPLA3 rs738409, and TM6SF2 rs58542926 variants were determined by allelic discrimination by predesigned Taqman assay (Applied Biosystems, Foster City, CA, EEUU) on DNA isolated. All SNPs were confirmed to be in Hardy-Weinberg equilibrium (figure 12).

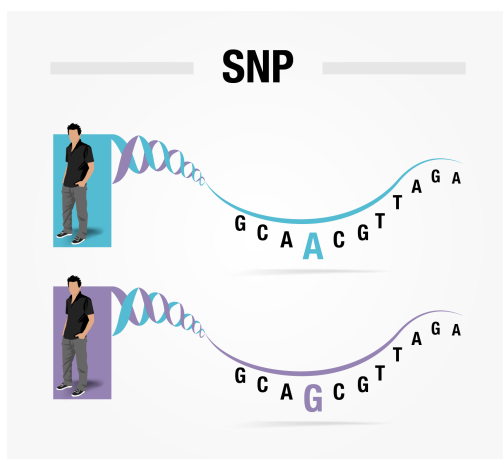


Figure 12. SNPs depiction.

5.5.3 Evaluation of FGF21 liver expression and peripheral mononuclear blood cells

Total RNA was isolated from 20 frozen human liver tissues using miRvana miRNA Isolation kit (Ambion, Life Technologies, USA) and mRNA levels were evaluated by quantitative real-time polymerase chain reactions (qRT-PCR). Ten patients presented NASH in liver biopsy and other ten just simple steatosis. Quantification of total RNA samples was determined by spectrophotometry using Qubit 2.0 (Invitrogen, Life Technologies, USA). RNA Integrity number (RIN) was measured by electrophoresis (Agilent Technologies, Inc.) to ensure the quality of samples. Cases presenting $RIN \leq 5$ were not suitable for the analysis. qRT-PCR reactions were carried out in triplicate (SensiFAST™ SYBR Lo-ROX One-Step Kit (Bioline, EEUU) in Eco™ Real-Time PCR System (illumina®, EEUU). RNA normalization was performed by amplification of *RNA 18S* as an endogenous control. The $2^{-\Delta\Delta CT}$ method was used for the analysis of the relative gene expression (106), and results were expressed as fold change.

Besides, total RNA from peripheral blood mononuclear cells (PBMC) was extracted from 30 patients (15 NASH and 15 simple steatosis) using TriZol Reagent (Invitrogen, Carlsbad, CA) and qRT-PCR was performed following the same protocol as described above.

5.5.4 Liver microRNAs isolation and quantification

Small RNA fraction, containing microRNAs profile, was isolated from 20 liver samples (10 presenting NASH and 10 displaying simple steatosis) by using miRvana™ miRNA Isolation kit (Ambion, Life Technologies, USA) (figure 13). This kit employs an organic extraction followed by immobilization of RNA on glass-fiber filters to purify either total RNA, or RNA enriched for small species, from cells or tissue samples. High yields of ultra-pure, high quality, small RNA molecules can be prepared in about 30 min. The sample is first lysed in a denaturing lysis solution, which stabilizes RNA and inactivates RNases. The

lysate is then extracted once with Acid-Phenol: Chloroform, which removes most of the other cellular components, leaving a semi-pure RNA sample. This is further purified over a glass-fiber filter by one of two procedures to yield either total RNA or a size fraction enriched in miRNAs. The glass-fiber filter method uses solutions formulated specifically for microRNA retention to avoid the loss of small RNAs that is typically seen with glass-fiber filter methods.

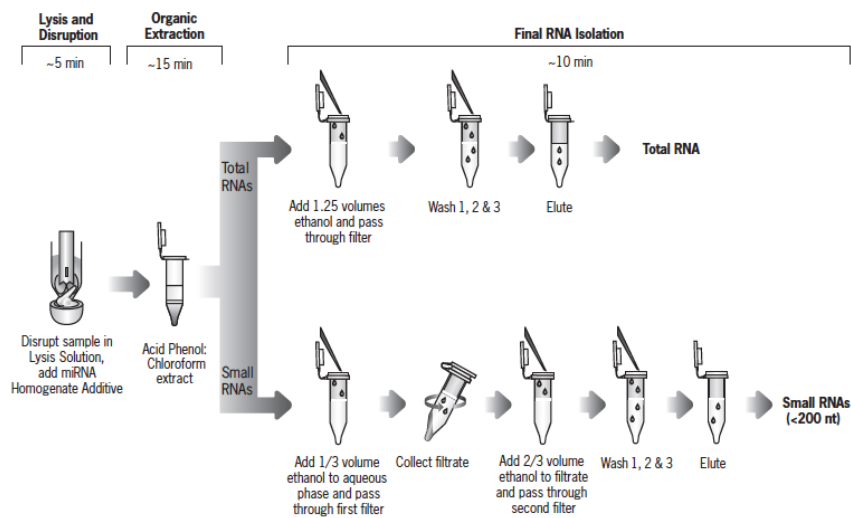


Figure 13. MiRvana™ isolation.

After assessment of the quality of samples (Agilent 2000 Bioanalyzer (Agilent Technologies, Inc.)), a screening of microRNAs with potential impact on the disease was performed. 96-wells miScript miRNA PCR Array Human Liver (QIAGEN, Hilden, Germany) was employed, for SYBR® Green-based, real-time PCR profiling of miRNAs (figure 14). This methodology uses mature miRNA-specific forward primers (miScript Primer Assays) that have been arrayed in biologically relevant pathway-focused, disease-focused, or whole miRNome panels.

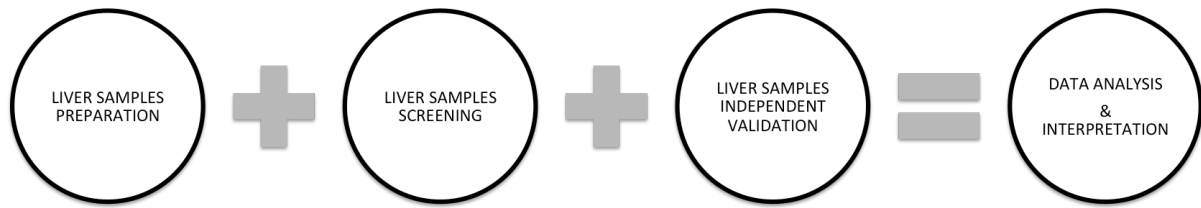


Figure 14. Liver samples methodology

Pooled cDNA at equal concentration were prepared according to two different conditions (NASH and SS) using the miScript II RT Kit and used as a template in real-time PCR with a miScript miRNA PCR Array and the miScript SYBR Green PCR Kit. Wells 1 to 84 each contain a miScript Primer Assay disease-related. Wells 85 and 86 contain replicate *C. elegans* miR-39 miScript Primer Assays that can be used as an alternative normalizer for array data. Wells 87 to 92 each include an assay for a different snoRNA/snRNA that can be utilized as a normalization control for the array data (figure 15).

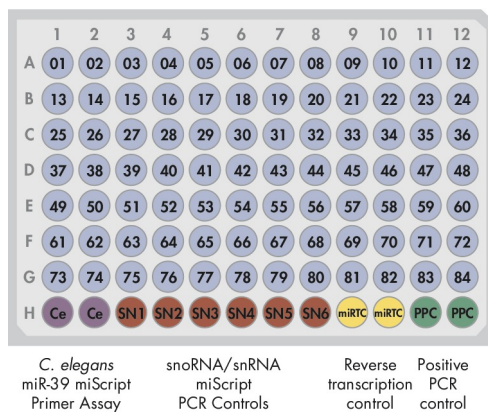


Figure 15. QIAgen predesigned array for candidates' evaluation.

After analysing the array layout, two candidates were identified and independently validated in liver samples. Thus, qRT-PCR reactions were carried out in triplicate using SNORD96A as endogenous control and hsa-miR-200b and hsa-miR-224 (QIAgen, Hilden,

Germany). cDNA synthesis was prepared from human liver tissues by using miScript reverse transcription kit (QIAGEN, Hilden, Germany) and qRT-PCR reactions were performed by miScript PCR kit.

5.5.5 Serum microRNAs isolation, quantification, and analysis

Further, to validate the potential of these microRNAs as surrogate biomarkers of the disease, small RNAs were isolated from 40 plasma samples, 20 from NASH patients and 20 with SS by using the miRNeasy mini kit (QIAGEN, Hilden, Germany) (figure 16). This kit combines phenol/guanidine-based lysis of samples and silica-membrane-based purification of total RNA. QIAzol Lysis Reagent is a monophasic solution of phenol and guanidine thiocyanate, designed to facilitate lysis, to denature protein complexes and RNases, and also to remove most of the residual DNA and proteins from the lysate by organic extraction. After addition of 200 μ L of sample per patients, QIAzol, and chloroform, the lysate is separated into aqueous and organic phases by centrifugation. RNA partitions to the upper, aqueous phase, while DNA partitions to the interphase and proteins to the lower, organic phase or the interphase. The upper, aqueous phase is extracted, and ethanol is added to provide appropriate binding conditions for all RNA molecules from approximately 18 nucleotides upwards. The sample is then applied to the RNeasy MinElute spin column, where the total RNA binds to the membrane and phenol and other contaminants are efficiently washed away. High-quality RNA is then eluted in a small volume of RNase-free water.

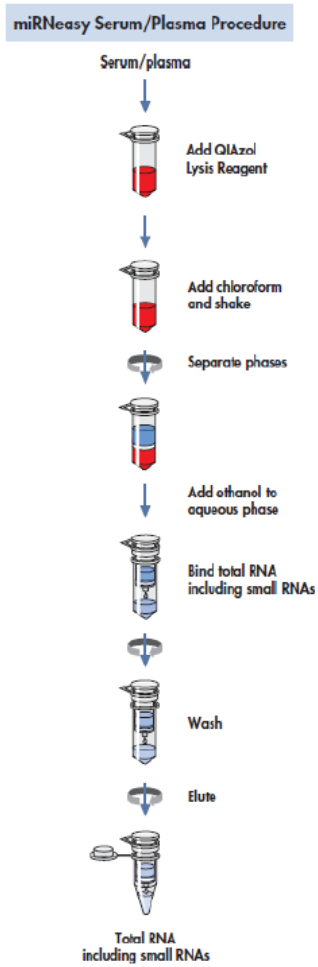


Figure 16. MiRNeasy Serum/plasma isolation procedure.

The quality of samples was further evaluated by NanoDrop™ 2000® (Wilmington, USA) to analyse the chemical interferences with QIAzol reagent. cDNA synthesis was prepared by using miScript reverse transcription kit (QIAGEN, Hilden, Germany) and PCR reactions were carried out in triplicate by using miScript PCR kit following manufacturer's instructions, using SNORD96A again as housekeeping gene.

5.6 Statistical analyses

Software package SPSS 22.0 (IBM, Chicago, IL, USA) was used to record data and to perform the detailed statistical analysis. Graphs were generated with both SPSS and Graph Pad Prism 6.0 (La Jolla, California). All p-values <0.05 were considered statistically significant. Normally distributed data are presented as mean \pm standard deviation (SD) and median (interquartile range) for non-normal continuous variables, whereas proportions were used for discrete variables.

5.6.1 Imaging biomarkers analysis

Receiver operating characteristics (ROC) curves, which represent the trade-off between the true and false-positive rates, were used to differentiate the misclassified data between normal and disease status. The statistical method to compare the area under the receiver operating characteristic (AUROC) curves was based on the method of Hanley et al (107, 108)

NASH and significant fibrosis (F2-F4) were dichotomised as presence or absence of the feature. NASHMRI and FibroMRI were the outputs of the optical analyses and were defined as predictive models to detect steatohepatitis and significant fibrosis. Multiple logistic regressions were performed to establish the final formula for NASH calculation (NASHMRI), and significant fibrosis (FibroMRI) presence. The sample size was intended to detect significant differences between histological diagnosis and NASHMRI and FibroMRI, using nQuery Advisor v7.0 software. Sample size of the validation cohort was 84 patients with a significance level (alpha) of 0.05, 1 – power (beta) of 0.20, prevalence of steatohepatitis of 0.5 and, under the hypothesis of AUROC curve, a difference <0.12 (i.e. AUROC for NASHMRI of 0.83 and for histological steatohepatitis of 0.95).

5.6.2 Genetic and epigenetic analysis

Statistical analyses using *t*-tests or ANOVA were carried out for normal distributions, and U-Mann Whitney or Kruskal-Wallis tests were carried out for non-normal variables. Categorical variables were explored by *X*-squared analysis, and finally, continuous variables were assessed by Pearson correlation coefficient. Independent variables were showing *p*-values ≤ 0.05 in univariate analysis were entered into backward Wald logistic regression analysis for genotyping evaluation, to escape from potentially confounding factors, to identify factors related to steatohepatitis and liver fibrosis. A multivariate model was constructed sequentially with variables entered one at the time, and a significance level of 0.05 was used to eliminate them from the model. Odds ratios (OR) and their 95% confidence intervals were estimated. The method used for missing data was complete-case analysis since statistical packages excluded individuals with any missing value. Serum *FGF21* levels were converted to natural logarithm to normalize data.

RESULTS

6.1 IMAGING BIOMARKERS

6.1.1 Development and standardisation of NASHMRI to detect steatohepatitis

One hundred and twenty-six patients were included on this analysis. Main characteristics of the overall cohort are summarized in table 6, and principal comparisons between estimation and validation cohorts in table 7.

Estimator E3 (harmonic mean) from MRI protocol SSFSE-T2, estimator E57 (second order contrast) from DYNAMIC MRI protocol, and estimator E73 (weighted mean curvature) from MRI protocol FAST-STIR, were found to be independently associated with NASH. Model coefficients associated with each one of these independent variables were $\beta_1=0.079$ (OR: 1.08, 95%CI: 1.02-1.15; $p=0.015$) and $\beta_2=0.127$ (OR: 1.14, 95%CI: 1.03-1.26; $p=0.015$). The influence of these estimators on the predictive equation to obtain the probability of suffering steatohepatitis was developed on estimation cohort and is given by:

$$\text{NASHMRI} = 1 / 1 + e^{1.654 - 0.079 * E3 (\text{SSFSE-T2}) - 0.127 * E57 (\text{DYNAMIC}) * E73 (\text{FAST-STIR})}$$

In the estimation cohort ($n=39$), AUROC obtained was 0.88 (95%CI: 0.77-0.99). Mean NASHMRI discriminated between simple steatosis and steatohepatitis, with high sensitivity (Se) and specificity (Sp). The best cut-off (based on Se and Sp) to segregate patients according to steatohepatitis presence or absence was 0.5; patients with a NASHMRI score > 0.5 were considered as NASH presence (figure 17). With this threshold, Se was 87%, Sp 74%, positive predictive value (PPV) 80% and negative predictive value (NPV) 82%.

In the validation cohort ($n=87$), NASHMRI AUROC obtained was 0.83 (95%CI: 0.75-0.92). Using the defined threshold of 0.5 for NASHMRI prediction, the results achieved were: Se 87%, Sp 60%, PPV 71% and NPV 81%.

Table 6. Baseline characteristics of the patient population: metabolic, demographic, and anthropometric data.

Parameter	Overall cohort (N=126)
Age; years	51±12
Male gender; %	78 (62%)
Body mass index; kg/m ²	30.6±4.8
Waist circumference; cm	102±11
Caucasian ethnicity; %	100
Arterial hypertension; %	36.4
Diabetes; %	37.5
Cholesterol; mmol/L	8.5±10.9
Triglycerides; mmol/L	5.9±11.7
ALT; IU/L	73±44
AST; IU/L	46±39
GGT; IU/L	101±101
Platelet count; x10 ⁹	233±57
Fasting glucose; mmol/L	5.6±3.8
HOMA index	3.8±2.8
Insulin; mg/dL	14.9±9.3
Albumin; g/dL	4.3±0.4
Sydney Index	0.31±0.31
NFS	-1.5±1.73
Transient elastography; kPa	7.6±6.1
CK-18; ng/ml	0.31±0.25
Liver biopsy length; mm	17.5±3.0

Table 7. Baseline characteristic comparisons between cohorts

Parameter	Overall Cohort (N=126)	Estimation Cohort (N=39)	Validation Cohort (N=87)	P
Age; years	51±12	52±11	50±13	ns
Male gender	83 (66%)	29/39 (74%)	54 (62%)	ns
BMI; Kg/m ²	30.6±4.8	29.2±4.8	31.1±5.1	ns
Steatosis grade; %				ns
1	75 (60%)	21 (54%)	54 (62%)	ns
2	31 (24%)	10 (26%)	21 (24%)	ns
3	20 (15%)	8 (21%)	12 (14%)	ns
NASH; %	65 (51%)	21 (54%)	44 (51%)	ns
Fibrosis stage; %				ns
F0	52 (41%)	13 (33%)	39 (44%)	ns
F1	24 (19%)	7 (18%)	17 (20%)	ns
F2	27 (21%)	9 (23%)	18 (21%)	ns
F3	16 (13%)	7 (18%)	9 (10%)	ns
F4	7 (6%)	3 (8%)	4 (5%)	ns

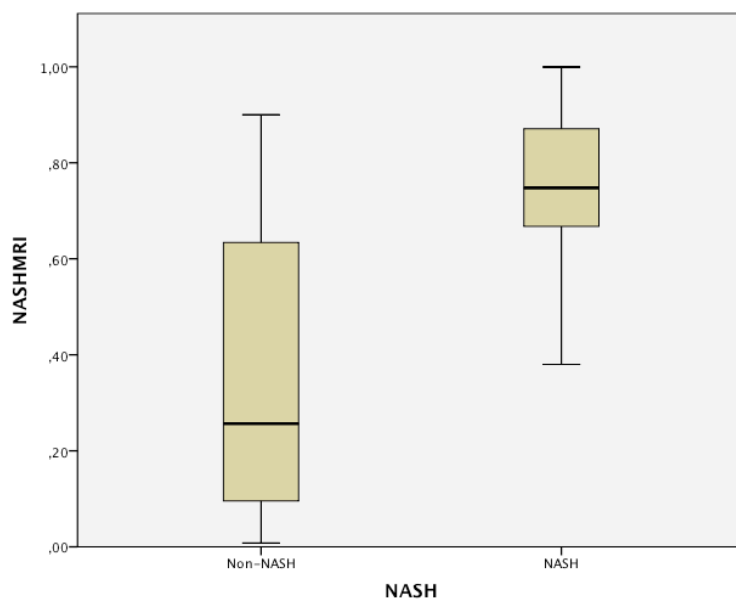


Figure 17. Box plot of NASHMRI according to NASH presence

6.2.2 Definition of FibroMRI for significant fibrosis prediction

Estimator E22 (Pearson's asymmetry coefficient) from MRI protocol SSFSE-T2 and estimators E3 (harmonic mean), E6 (mode), E31 (column's mean of multi-oriented co-occurrence matrix) and E75 (maximum of main curvatures) from MRI protocol DYNAMIC were found to be independently associated with fibrosis (table 8).

Model coefficients associated with each of these independent variables were: $\beta_1=1.101$ (OR: 3.01, 95%CI: 1.25-7.25; $p=0.014$); $\beta_2= -1.105$ (OR: 0.33, 95%CI: 0.14-0.77; $p=0.010$); $\beta_3= -115.737$ (OR: 0.08, 95%CI: 0.02-0.14; $p=0.046$); $\beta_4=0.696$ (OR: 2.00, 95%CI: 1.19-3.38; $p=0.009$); and $\beta_5= -0.825$ (OR: 0.44, 95CI%: 0.21-0.93; $p=0.030$). Their introduction into the predictive equation defining the risk of suffering fibrosis was:

$$\text{Fibro-MRI} = 1 / (1 + e^{-4.207 - 1.101 * E3 \text{ (DYNAMIC)} + 1.105 * E6 \text{ (DYNAMIC)} + 115.737 * E22 \text{ (SSFSET2)} - 0.696 * E31 \text{ (DYNAMIC)} + 0.825 * E75 \text{ (DYNAMIC)})}$$

In the estimation cohort ($n=39$), AUROC obtained was 0.94 (95%CI: 0.87-1.00). FibroMRI differentiated between mild (F0-F1) and significant (F2-F3-F4) fibrosis, without any overlap. The best cut-off, determined by Se and Sp, to segregate patients with absence or presence of significant fibrosis was 0.5; those patients with a FibroMRI > 0.5 were considered as suffering from significant fibrosis (figure 18). With the previously defined cut-off point of 0.5 for FibroMRI, the results obtained were: Se 81%, Sp 85%, PPV 77% and NPV 86%. In the validation cohort ($n=87$), FibroMRI AUROC for significant fibrosis was 0.85 (95%CI: 0.77-0.93). With the defined threshold at 0.5 for FibroMRI prediction, the results obtained were: Se 77%, Sp 80%, PPV 67% and NPV 87%.

Table 8: Definition and properties of the estimators

PROTOCOL	ESTIMATOR	NAME	DEFINITION AND PROPERTIES
SSFSE-T2	E3	Harmonic mean	The harmonic mean of a set of values, in this case, the set of pixels of a sample, is a special type of media used when the average of rates is desired. The harmonic mean is the reciprocal of the arithmetic mean of the reciprocals
DYNAMIC	E57	Second order contrast	Another texture attribute of a given sample, computed as a local grey level variation in the grey level co-occurrence matrix. It can be thought of as a linear dependency of grey levels of neighbouring pixels. If the neighbouring pixels are very similar in their grey level values then the contrast in the image is very low. In case of texture, the grey level variations show the variation of texture itself. High contrast values are expected for heavy textures and low for smooth, soft textures
FAST-STIR	E73	Weighted mean curvature	Curvature is a feature used to describe image surface. The Weighted mean curvature is a value representing the mean of the curvatures mean at each pixel within the image sample.
SSFSE-T2	E22	Pearson's asymmetry coefficient	Pearson's asymmetry coefficient, also called Pearson's first coefficient of skewness, is a way to figure out the skewness of a distribution. It tells how far the distribution departs from symmetry.
DYNAMIC	E6	Mode	The Mode of a set of numbers, in this case the pixel sample values, is the value that occurs most often.
DYNAMIC	E31	Column's mean of multi-oriented co-occurrence matrix	In image processing, co-occurrence matrices are used to analyse the texture of an image. A multi-oriented matrix computes the magnitude and orientation of the local gradient vector at each pixel position, so each pixel carries its grey value, its gradient magnitude and its gradient orientation.
DYNAMIC	E75	Maximum of main curvatures	In this case, the maximum value for all the primary curvatures (primary curvature from every pixel of the sample) is used as a surface attribute descriptor.

Number of patients suffering from advanced fibrosis and/or cirrhosis was not enough to define outright thresholds beyond significant fibrosis. Nevertheless, FibroMRI correlated with fibrosis stage ($r=0.54;p<0.0001$), independently of device used (General Electrics (GE) $r=0.54;p<0.001$ and Philips $r=0.44;p<0.002$). Finally, FibroMRI was found different according to the stage of fibrosis: F0 (n=36) 0.16 ± 0.24 [95%CI 0.07-0.24]; F1 (n=16) 0.34 ± 0.40 [95%CI 0.12-0.55] and $F\geq 2$ (n=30) 0.64 ± 0.30 [95%CI 0.53-0.75]; $p<0.0001$.

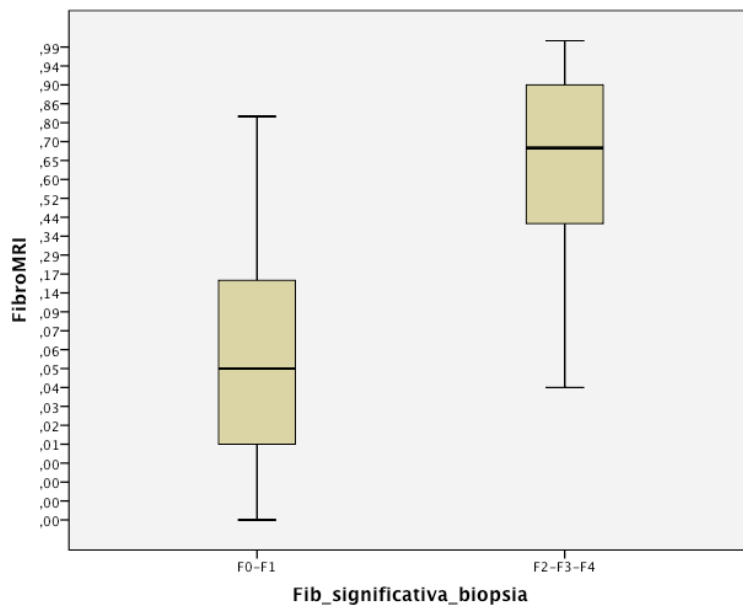


Figure 18. Box plot of FibroMRI according to significant fibrosis detection.

6.2.3. Comparative analyses of NASHMRI and FibroMRI

6.2.3.1 Standardisation of NASHMRI and FibroMRI across MRI systems

NASHMRI calculated using GE scanners (n=35) showed a similar diagnostic accuracy when compared with NASHMRI calculated in patients who underwent MRI using the Philips system (n=52) i.e. AUROC=0.75 (95%CI: 0.56-0.95) vs. AUROC=0.85 (95%CI: 0.73-0.97), respectively ($p=ns$). Regarding FibroMRI, evaluations performed using GE MRI scanners showed an AUROC of 0.80 (95%CI: 0.65-0.95) vs. AUROC of 0.84 (95%CI: 0.72-0.96) using the Philips system ($p=ns$). Scores yielded by both scanners are comparable, and

the same thresholds for NASHMRI and FibroMRI applied to both devices (GE or Philips). Spearman coefficient together with diagnostic accuracy was similar for both scanners and end-points.

Both machines pose the same image quality and resolution and were processed likewise with FibroMRI and NASHMRI without distinctions. In a subset of 9 patients, both studies were available (6 w/o fibrosis and 5 w/o NASH). Fibrosis was detected by both methods in 3/3 cases and excluded fibrosis in 5/6 cases without this condition using both Philips and GE devices. Besides, NASH was confirmed in 3/4 cases by both techniques and excluded in 4/5 cases. Further analysis including a large cohort of patients would better define the reproducibility of these results.

6.2.3.2. Comparative analysis with non-invasive biochemical markers of steatohepatitis

NASHMRI was compared with CK-18 levels in NASH diagnosis. NASHMRI offered the best diagnostic accuracy with an AUROC of 0.86 (95%CI: 0.76-0.96) for steatohepatitis presence. This was significantly better than CK-18 levels, which showed an AUROC of 0.56 (95%CI: 0.40-0.71; $p<0.05$) (Figure 1). NAS score correlated significantly with NASHMRI ($r=0.38$; $p<0.001$) and CK-18 levels ($r=0.29$; $p<0.02$) (figure 19)

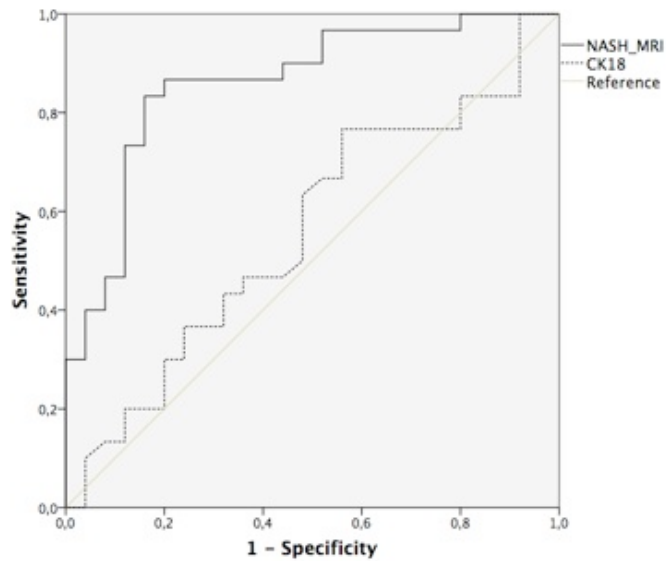


Figure 19. Analysis of diagnostic accuracy for NASH detection comparing NASHMRI and CK-18.

6.2.3.3. Comparative analysis with non-invasive biochemical markers of significant fibrosis

FibroMRI was significantly superior to NFS and Sydney Index (AUROC: 0.85; 95%CI: 0.74-0.97 vs. AUROC: 0.76; 95%CI: 0.61-0.91 vs. AUROC: 0.69; 95%CI: 0.50-0.87, respectively; $p < 0.05$) in predicting significant fibrosis. Fibrosis stage correlated with FibroMRI ($r = 0.61$; $p < 0.001$), and NFS ($r = 0.52$; $p < 0.001$). Also, a significant correlation between NFS and FibroMRI was observed ($r = 0.53$; $p < 0.001$) (figure 20).

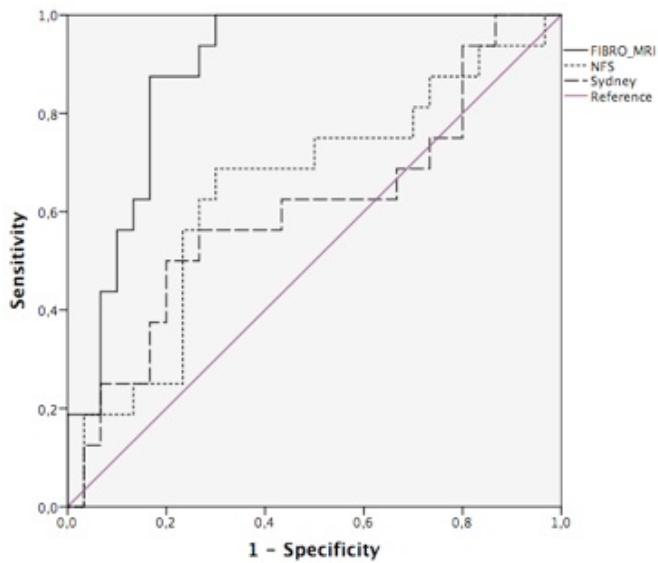


Figure 20. Analysis of diagnostic accuracy for significant fibrosis ($\geq F2$) comparing FibroMRI, Sydney Index and NAFLD Fibrosis Score.

Lastly, findings with FibroMRI were similar to that of transient elastography (AUROC: 0.95; 95%CI: 0.88-1.00 vs. AUROC: 0.91; 95%CI: 0.81-1.00, respectively; $p=ns$) (figure 21).

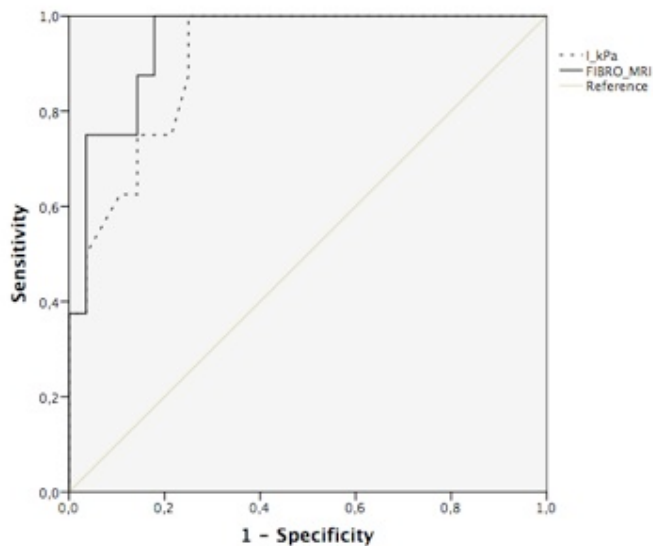


Figure 21. Analysis of diagnostic accuracy for significant fibrosis ($\geq F2$) detection comparing Fibro-MRI and valid transient elastography measurements.

6.2 GENETIC AND EPIGENETIC BIOMARKERS

6.2.1 Hepatic *FGF21* expression is increased in NASH patients

Main characteristics of this substudy cohort are summarized in table 9.

Table 9. Main features of the group of patients analysed.

VARIABLE	Cohort (N=20)
Age (years)	46.2±9.7
Gender (male/female)	60%/40%
BMI (kg/m ²)	28.45±4.71
Diabetes mellitus (%)	25% (5/20)
Arterial hypertension (%)	20% (4/20)
HOMA-IR	3.6±2.6
ALT (IU/mL)	48.7±25.1
AST (IU/mL)	34.3±17.3
GGT (IU/mL)	120.7±122.9
NASH (%)	50% (10/20)
Significant fibrosis (F2-F4) (%)	10% (2/20)
Steatosis, presence (%)	55% (11/20)
Ballooning degeneration, presence (%)	30% (6/20)

Quantitative RT-PCR analysis showed that hepatic *FGF21* expression was increased in individuals presenting NASH and inhibited in simple steatosis (fold change 3.45±4.0 vs. 0.63±0.90, p=0.002) (figure 23). *RNA 18S* expression was observed in control samples, with positive amplification at cycle 10, and *FGF21* expression was detected at cycle 28.

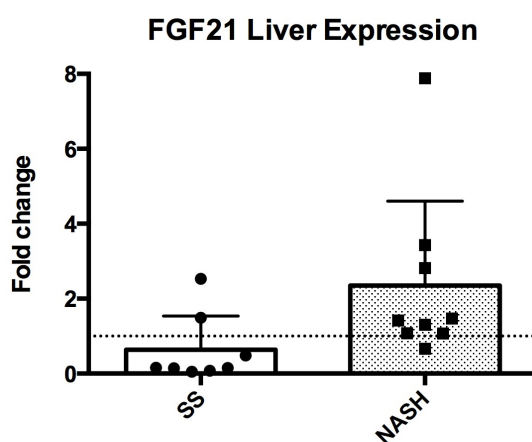
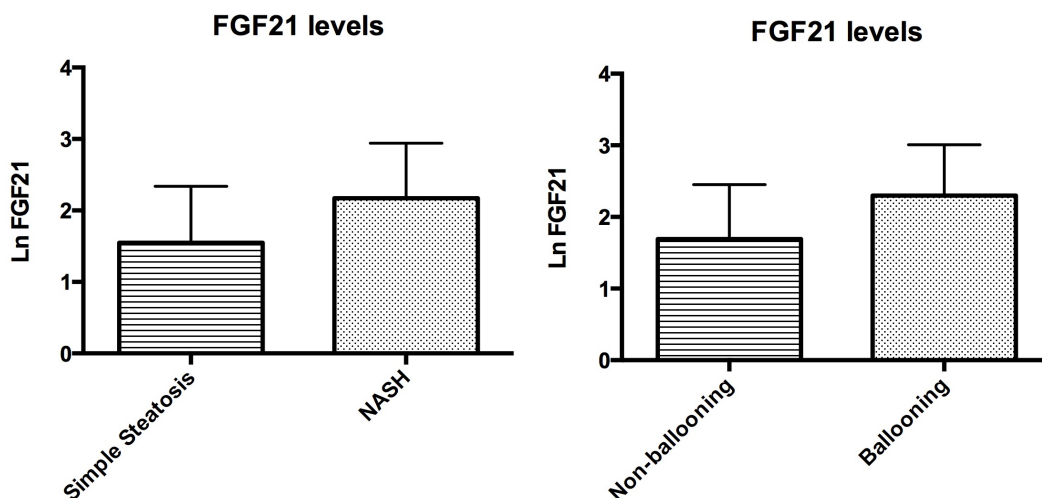


Figure 23. Liver *FGF21* expression

Further, a significant correlation was found between *FGF21* mRNA levels and BMI ($r=0.736$, $n=14$; $p=0.004$), endogenous insulin levels ($r=0.613$, $n=14$; $p=0.02$), HOMA-IR ($r=0.552$, $n=14$; $p=0.041$) and transient elastography ($r=0.687$, $n=10$; $p=0.028$). PBMC were also analysed for *FGF21* mRNA abundance, but no PCR products were detected by qRT-PCR analysis.

6.2.2 Serum *FGF21* levels are increased in advanced NAFLD

Thirty-eight patients were examined, nineteen showing NASH at liver biopsy and other nineteen just simple steatosis. No patient presented serum *FGF21* levels below quantification limit. Correlation analyses were performed between serum *FGF21* levels and several anthropometric and metabolic characteristics of patients. NASH patients showed increased serum *FGF21* levels compared to non-NASH subjects (2.17 ± 0.77 vs. 1.55 ± 0.79 ; $p=0.025$). Moreover, patients suffering from hepatocellular ballooning showed higher levels of *FGF21* than patients without it (2.30 ± 0.71 vs. 1.69 ± 0.76 , $p=0.045$). Finally, *FGF21* levels were also significantly correlated with NAS Score ($r=0.364$, $n=37$, $p=0.027$) (figures 24 and 25).



Figures 24 and 25. *FGF21* levels according to NASH and hepatocellular ballooning.

Furthermore, consistently with *FGF21* mRNA expression, protein production was increased in patients with advanced fibrosis (F3-F4) vs. mild fibrosis (F0-F1-F2) (2.18 ± 0.77 vs. 1.75 ± 0.79 ; $p=ns$) but not statistically significant.

6.2.3 Bearing GG genotype from PNPLA3 rs738409 confers susceptibility to NASH development

First, two hundred and twenty five biopsy-proven NAFLD patients, mean age 47 years and almost 60% female composed this cohort. Main clinical and epidemiological characteristics of the overall cohort are provided in Table 10. Up to 31% of patients showed NASH in liver biopsy and more than 22% significant fibrosis stages (F2-F4) (table 10).

Table 10. Baseline characteristics of the patient population: metabolic, demographic, and anthropometric data.

VARIABLE	Overall cohort (N=225)
Age (years)	47.4 \pm 13.2
Gender (male/female)	42%/58%
BMI (kg/m²)	32.2 \pm 9.1
Diabetes mellitus (%)	16.4% (37/225)
Arterial hypertension (%)	24% (54/225)
HOMA-IR	3.5 \pm 4.6
Glucose (mg/dL)	100.45 \pm 28.6
Insulin (microUI/mL)	13.14 \pm 12.77
ALT (IU/mL)	43.3 \pm 35.6
AST (IU/mL)	32.2 \pm 27.1
GGT (IU/mL)	72.1 \pm 101.5
Alkaline phosphatase (IU/mL)	77.7 \pm 31.4
Total cholesterol (mg/dL)	197.7 \pm 41.8
HDL-c (mg/dL)	49.9 \pm 17.5
LDL-c (mg/dL)	123.5 \pm 36.6
Triglycerides (mg/dL)	139.3 \pm 82.3
NASH (%)	31.1% (52/167)
Significant fibrosis (F2-F4) (%)	22.2% (50/225)
Advanced fibrosis (F3-F4) (%)	10.7% (24/225)
<i>FGF21</i> rs838133 variant, AA genotype (%)	20.9% (47/225)
<i>FGF21</i> rs838133 variant, AG genotype (%)	47.1% (106/225)
<i>FGF21</i> rs838133 variant, A allele (%)	68% (153/225)

In univariate analysis, gender, BMI higher than 25 kg/m², diabetes mellitus type 2, AST, ALT glucose, insulin, HOMA-IR, triglycerides and GG genotype from PNPLA3 were found statistically associated with NASH.

Further, in multivariate analysis, gender [OR 2.74 (95% CI 1.18-6.93), p=0.019], HOMA-IR [OR 1.526 (95% CI 1.25-1.85), p=0.000] and carrying GG genotype of PNPLA3 [OR 3.020 [95% CI 1.17-7.73], p=0.021] were found as variables independently associated with NASH (table 11).

Table 11. Univariate and multivariate analyses according to NASH (N=200).

Variable	Univariate analysis			Multivariate analysis	
	Simple Steatosis (n=137)	NASH (n=63)	p-value	OR [95%CI]	p-value
Gender distribution (Males vs females, %)	23.1 %	41.3 %	0.006	OR 2.74 [95% CI 1.18-6.93]	0.019
BMI>25 kg/m ²	11.8 %	33.1 %	0.014		
Age (years)	46.3	49.9	0.098		
T2DM (diabetic vs non-diabetic)	23.9%	62.9%	0.000		
AST (IU/mL)	27.4	45.9	0.000		
ALT (IU/mL)	34.2	70.1	0.000		
GGT (IU/mL)	64.4	105.5	0.057		
Glucose (mg/dL)	95.6	110.8	0.001		
Insulin (mg/dL)	9.8	21.4	0.000		
HOMA-IR	2.4	6.3	0.001	OR 1.53 [95% CI 1.25-1.85]	0.000
Triglycerides (mg/dL)	122.4	159.3	0.012		
Total cholesterol (mg/dL)	199.51	199.51	0.988		
LDL-cholesterol (mg/dL)	117.4	129.7	0.179		
HDL-cholesterol (mg/dL)	53.8	46.0	0.517		
Total bilirubin	0.58	0.64	0.517		
Alkaline phosphatase (IU/mL)	76.9	80.7	0.470		
Albumin (mg/dL)	4193	4253	0.581		
Platelet count (x10 ⁹)	241.5	223.3	0.113		
Haemoglobin (g/dL)	14.22	14.12	0.798		
Cholinesterase	11462.2	9655.8	0.565		
HTA	29.5%	35.2%	0.443		
FGF21 (GA/AA vs GG)	22.6 %;	26.9 %	0.545		
PNPLA3 (GG vs CG/CC)	24.5 %	51.4 %	0.002	OR 3.02 [95% CI 1.17-7.73]	0.021
TM6SF2 (CT/TT vs CC)	29.9%	32.0 %	0.835		

Combining those parameters, AUROC obtained for NASH prediction was AUROC: 0.833 [95% CI 0.767-0.900]; p=0.000 (figure 26).

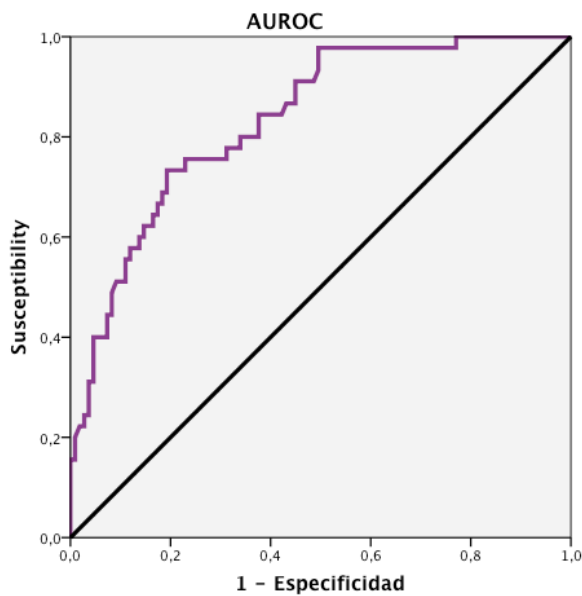


Figure 26. AUROC for NASH prediction

6.2.4 Carrying A-allele from FGF21 rs838133 confers susceptibility to significant fibrosis

In univariate analysis, *FGF21* rs838133 A-allele (AA/AG 27.5% (42/153) vs. GG 11.1% (8/72); p=0.006) was determined as a risk factor for significant fibrosis (F2-F3-F4). *PNPLA3* gene was also found associated with significant fibrosis (GG 32.6% (15/46) vs. GC/CC 20.1% (36/179); p=0.040). Further variables associated with significant fibrosis were male gender, age at liver biopsy, BMI \geq 25 kg/m², type 2 diabetes mellitus, AST, ALT, GGT, insulin, glucose, HOMA-IR, triglycerides, and platelets.

Besides, in multivariate analysis, variables independently associated with significant fibrosis were: A-allele of *FGF21* rs838133 [OR 3.91 (95% CI 1.09-14.06); p=0.006]; age [OR 1.07 (95% CI 1.03-1.11); p=0.001]; type 2 diabetes mellitus [OR 4.08 (95% CI 1.51-10.97); p=0.005] and ALT [OR 1.03 (95% CI 1.01-1.04); p=0.000] (table 12).

Table 12. Univariate and multivariate analyses according to significant fibrosis stages (N=225).

Variable	Univariate analysis			Multivariate analysis	
	Mild fibrosis (F0-F1) (n=175)	Significant fibrosis (F2-F3-F4) (n=50)	p-value	OR [95%CI]	p-value
Gender distribution (Males vs females, %)	19.1 %	30.0 %	0.040		
BMI>25 kg/m ²	4.4 %	25.3 %	0.002		
Age (years)	45.9	52.1	0.002	OR 1.07 [95% CI 1.03-1.11]	0.001
T2DM (diabetic vs non-diabetic)	15.8%	46.8%	0.000	OR 4.08 [95% CI 1.51-10.97]	0.005
AST (IU/mL)	27.6	47.7	0.000		
ALT (IU/mL)	36.3	67.5	0.000	OR 1.03 [95% CI 1.01-1.04]	0.000
GGT (IU/mL)	67.1	108.2	0.054		
Glucose (mg/dL)	95.2	118.1	0.001		
Insulin (mg/dL)	10.3	23.6	0.000		
HOMA-IR	2.4	7.1	0.000		
Triglycerides (mg/dL)	122.4	159.3	0.012		
Total cholesterol (mg/dL)	196.6	201.9	0.449		
LDL-cholesterol (mg/dL)	113.2	129.3	0.179		
HDL-cholesterol (mg/dL)	50.3	48.6	0.539		
Total bilirubin	0.60	0.61	0.922		
Alkaline phosphatase (IU/mL)	76.6	87.7	0.300		
Albumin (mg/dL)	4188.0	4349.2	0.060		
Platelet count (x10 ⁹)	243.2	213.9	0.006		
Haemoglobin (g/dL)	14.1	14.3	0.564		
Cholinesterase	11462.2	9655.8	0.565		
HTA	19.6%	28.4%	0.126		
FGF21 (AA vs AG/GG)	11.1 %;	27.5 %	0.006	OR 3.91 [95% CI 1.09-14.06]	0.037
PNPLA3 (GG vs CG/CC)	20.1 %	32.6 %	0.040		
TM6SF2 (CT/TT vs CC)	20.7 %	29.0 %	p=0.295		

Further, AUROC for significant fibrosis prediction was calculated, reaching 0.89 [95% CI 0.85-0.95] (figure 27).

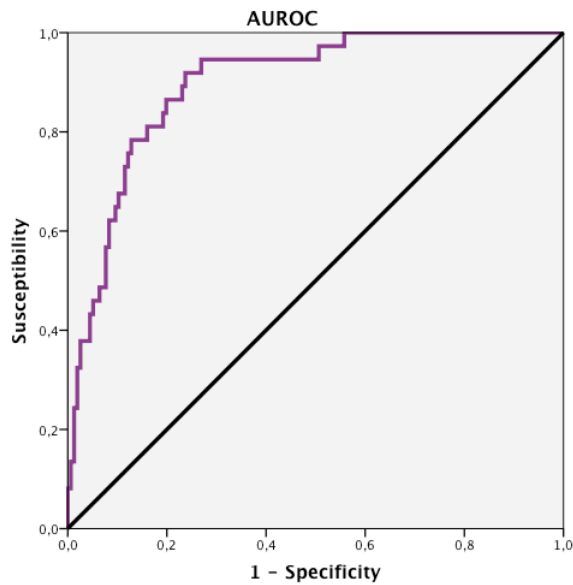


Figure 27. AUROC obtained for significant fibrosis prediction.

Lastly, formulas employed to obtain those AUROCs for both NASH and significant fibrosis prediction were the following:

$$\text{NASH} = 1 / 1 + e^{(-3.083 - 1.101 * \text{GENDER}) + 1.105 * \text{GG GENOTYPE PNPLA3} + 0.423 * \text{HOMA-IR}}$$

$$\text{Significant fibrosis} = 1 / 1 + e^{(-5.480 - 0.031 * \text{AGE} + 1.587 * \text{DM2} + 0.024 * \text{ALT} - 1.325 * \text{A-ALLELE FGF21})}$$

6.2.5 Identification of target microRNAs: miR-200b-3p and miR-224-5p

Two candidates (miR-200b-3p and miR-224-5p) were identified after obtaining the results of the predesigned array. In this pooled analysis, miR-200b-3p was found 2.8-fold overexpressed in NASH patients vs. SS, as well as miR-224 reached 3.09-fold (figure 28).

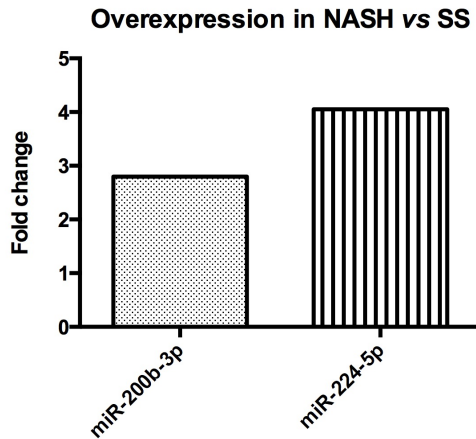
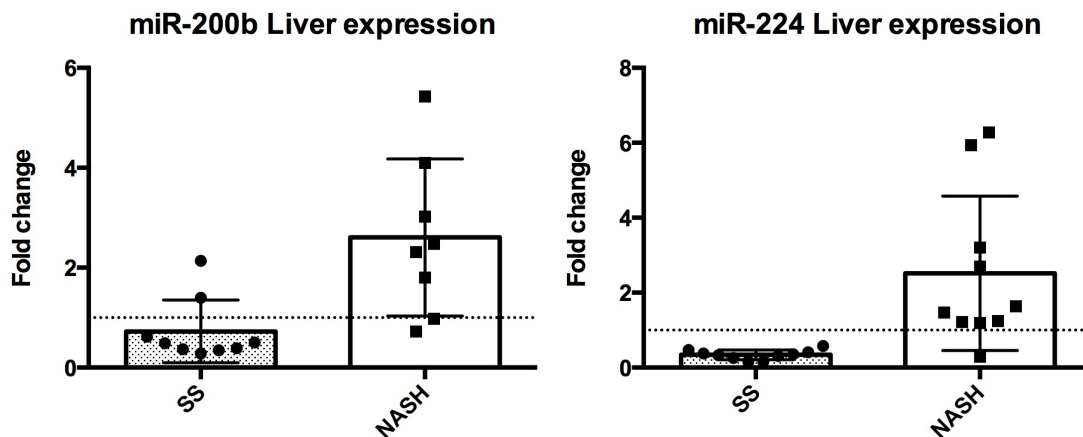


Figure 28. Target microRNAs findings in pool of NASH vs. SS

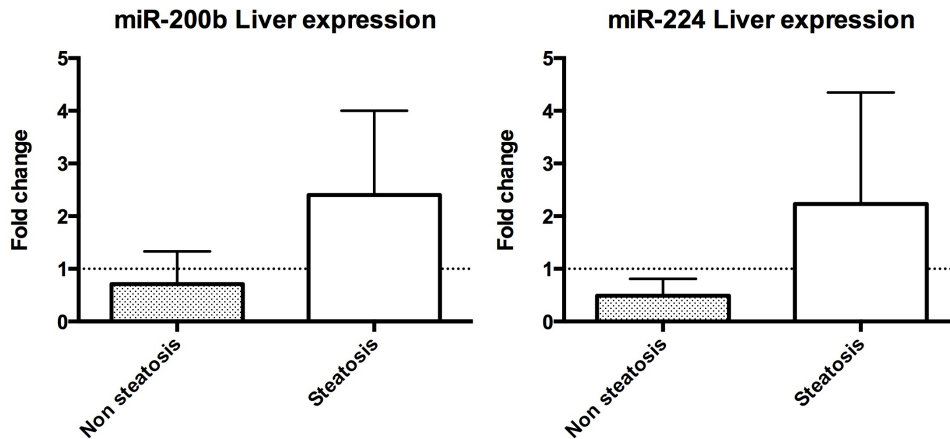
6.2.6 Both liver miR-200b and miR-224 are induced in NASH, steatosis and ballooning.

Both liver miR-200b and miR-224 expression were found upregulated in NASH vs SS patients [2.60 ± 1.57 vs 0.72 ± 0.62 , $p=0.0016$ and 2.51 ± 2.06 vs 0.34 ± 0.13 , $p=0.0005$ respectively] (figures 29 and 30).



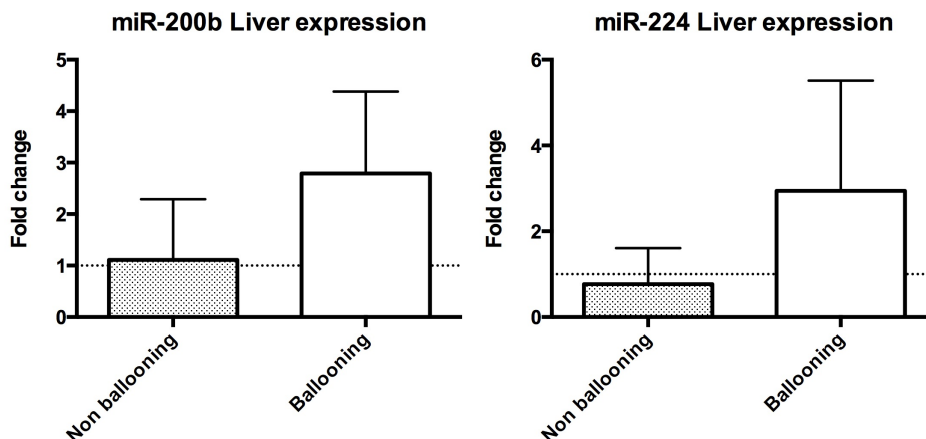
Figures 29 and 30. Liver miR-200b and liver miR-224 according to NASH.

Besides, both miR-200b and miR-224 were associated with steatosis presence in liver biopsy [2.40 ± 1.60 vs 0.71 ± 0.62 , $p=0.009$ and 2.23 ± 2.12 vs 0.49 ± 0.32 , $p=0.014$] (figures 31 and 32).



Figures 31 and 32. MiRNAs liver expression according to presence or absence of steatosis.

Further, both miRNAs were found associated with ballooning degeneration [2.79 ± 1.59 vs 1.11 ± 1.18 , $p=0.027$ and 2.94 ± 2.57 vs 0.77 ± 0.84 , $p=0.048$] (figures 33 and 34).



Figures 33 and 34. MiRNAs liver expression according to ballooning.

Finally, liver miR-200b was found associated with age [$r=0.708$, $p=0.001$, $n=17$], HOMA-IR [$r=0.567$, $p=0.028$, $n=15$] and BMI [$r=0.647$, $p=0.005$, $n=17$], as well as liver miR-224 expression was associated with age [$r=0.582$, $p=0.009$, $n=19$], HOMA-IR [$r=0.614$, $p=0.011$, $n=19$] and BMI [$r=0.612$, $p=0.009$, $n=19$].

6.2.7 Plasma miR-200b and miR-224 are induced in NASH but not in significant fibrosis, steatosis or ballooning

Forty NAFLD biopsy-proven NAFLD patients, mean age around 50 years old, 60% male and 5% with NASH composed this substudy (table 13).

Table 13. Main features of the group of patients analysed

VARIABLE	Cohort (N=40)
Age (years)	49.7 \pm 10.1
Gender (male/female)	60%/40%
BMI (kg/m²)	31.40 \pm 5.31
Diabetes mellitus (%)	37.5%
Arterial hypertension (%)	25%
HOMA-IR	5.5 \pm 2.1
ALT (IU/mL)	52.4 \pm 32.4
AST (IU/mL)	37.6 \pm 23.4
GGT (IU/mL)	78.9 \pm 102.3
NASH (%)	50%
Significant fibrosis (F2-F4) (%)	30%
Steatosis, presence (%)	75%
Ballooning degeneration, presence (%)	26%

In plasma of patients with NASH miR-200b was found increased vs simple steatosis individuals (fold change 2.00 \pm 1.30 vs 0.96 \pm 1.09; $p=0.03$) (figure 35), but not with significant fibrosis stages ($p=0.6$), steatosis presence ($p=0.49$) or ballooning ($p=0.38$).

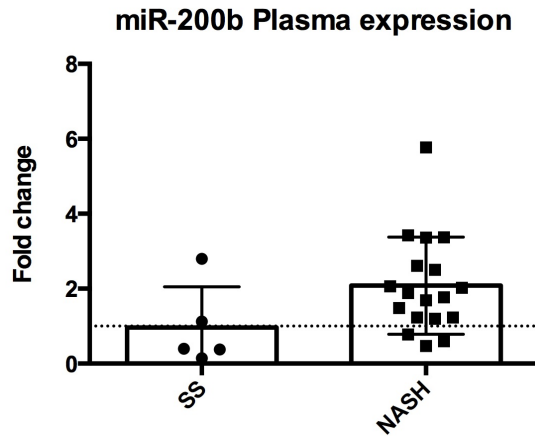


Figure 35. MiR-200b plasma expression according to NASH

Further, miR-224 was found upregulated in NASH vs SS (fold change 1.60 ± 1.52 vs 0.26 ± 0.32 ; $p=0.002$) (figure 36), but again not in significant fibrosis patients ($p=0.20$) or steatosis presence ($p=0.37$). It was observed a clear trend among presence or absence of ballooning, but it did not reach statistical significance (1.70 ± 1.93 vs. 0.90 ± 1.10 ; $p=0.20$).

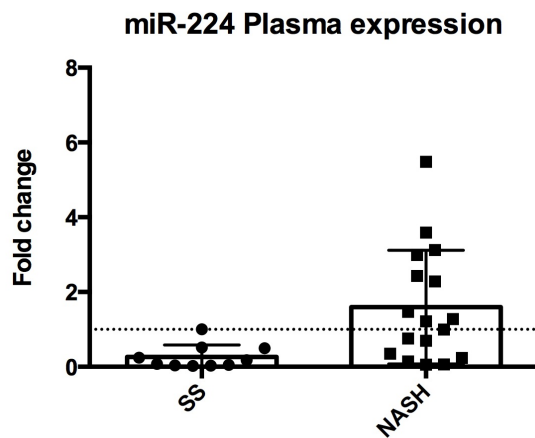


Figure 36. MiR-224 plasma expression according to NASH.

Finally, both AUROCs were calculated for NASH prediction. First, AUROC obtained to predict NASH by using miR-200b was 0.800 [95%CI 0.522-1.000; p=0.43] (figure 37).

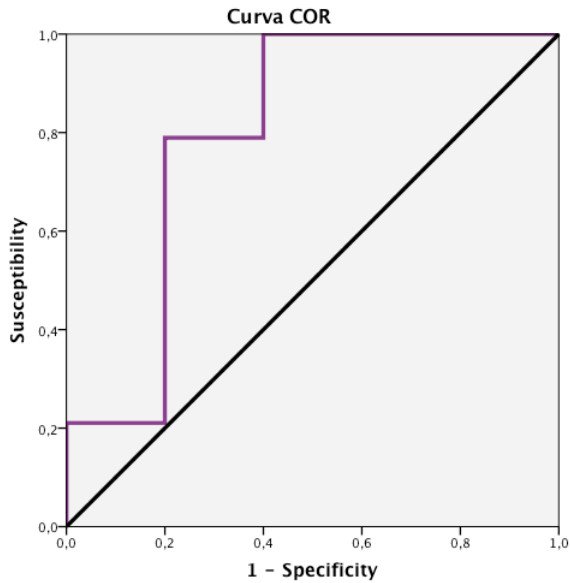


Figure 37. AUROC for NASH prediction using plasma expression of miR-200b.

Furthermore, AUROC reached for NASH prediction by using miR-224 was slightly superior, 0.84 [95% CI 0.694-0.988; p=0.004] (figure 38).

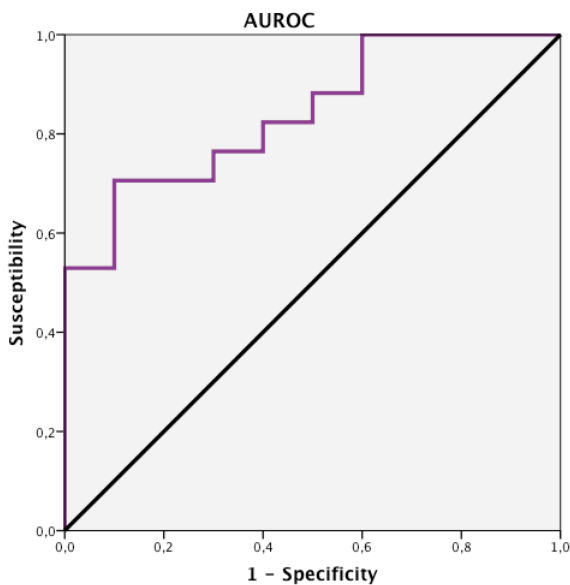


Figure 38. AUROC for NASH prediction using plasma expression of miR-224.

DISCUSSION

NAFLD is the fastest rising cause of hepatic disease worldwide, with no signs of decline. Significant progress has been achieved over the past decade regarding the pathophysiology and natural history of this disease, discovering that necroinflammation and fibrosis are the features that have worse prognosis. These methods have gained popularity among clinicians, and given the high prevalence of this disease in general population; the need for a definite approach is more urgent.

Computerised optical analysis of conventional non-contrast-enhanced MR images of the liver enables the detection of steatohepatitis by NASHMRI and significant fibrosis by FibroMRI in patients suffering from NAFLD. This study addresses a critical need for non-invasive markers of both NASH and the associated fibrosis. Since fibrosis and steatohepatitis generate appreciable architectural changes in liver structure, it would be possible, using this software, to forecast the rate of disease progression, to support therapeutic decision-making, and to monitor potential effects of therapy.

Diagnoses of liver diseases have long relied on liver biopsy, despite their high intra- and inter-observer variability, discomfort to the patient, and sampling error (32). A panel of serum biomarkers to confirm, or rule out, steatohepatitis has remained elusive. To date, panels of serum biomarkers for non-invasive assessment have been used as surrogate measures. Nevertheless, these methods show many limitations, like fluctuations during concomitant disease or lack of reproducibility that could translate to false estimation of the disease. Furthermore, these panels are not able to monitor disease progression, due to their accuracy being hindered by inflammation.

One of the major drawbacks of serum biomarkers is its availability for routine

clinical use. In an analysis to determine the most cost-effective non-invasive screening strategies in a general population vs a high-risk population, that compared NAFLD fibrosis Score, TE, ARFI, CK-18 for detecting fibrosis and NASH, it was shown that screening with the NAFLD fibrosis score/TE/CK-18 algorithm was the most appropriate in high-risk obese or diabetic patients (109). The NashTest, included in FibroMax® (110), is a semi-quantitative score with a wide grey zone, and OWLiver® (111) accurately predicts steatohepatitis. However, it needs to be analysed in a centralised laboratory, and which undermines its accessibility.

Non-invasive diagnosis of significant fibrosis in NAFLD is also a challenge. NAFLD Fibrosis Score was specifically developed for NAFLD. However, it showed a wide grey zone in the validation process. Non-invasive markers shunted from hepatitis C evaluations have been tested in NAFLD. These include Sydney, FIB-4, Forns and APRI indices. However, poor correlations between serum biomarkers of liver fibrosis (APRI, FIB-4, AST/ALT ratio, European Liver Panel and Liver stiffness measurement) were reported in diabetic patients. The agreement was good on absence of advanced liver disease, but not in patients with progressive disorders. FibroMRI was superior to NFS and Sydney Index in predicting significant fibrosis. These results would be expected because NFS was designed to predict advanced fibrosis from significant fibrosis, and Sydney Index was developed in patients with chronic hepatitis C. So these scoring systems based on routine lab work, such as FIB-4, NFS, APRI, Forns and BARD indexes could be easily calculated at the bedside and can accurately identify patients at a higher risk of liver-related complications, death or transplantation.

However, experts agree that these surrogate biomarkers could rapidly evolve and be readily applied to routine clinical practice in the advancing area of NAFLD, especially in at-risk populations. Currently, clinical trials are limited by the lack of a

non-invasive method with high diagnostic accuracy, reliability, feasibility, cost-effectiveness and able to measure the responsiveness of treatment.

Image-based non-invasive methods are receiving increasing attention. They have shown a satisfactory correlation with fibrosis staging, but still, need suitable validation before being used to guide therapies. For liver fat content quantification, CAP is simple and accurate but needs to be implemented with the XL probe to ensure the diagnosis in NAFLD patients. Therefore, despite its limitations, US remains the most widely used tool in clinical practice.

Ultrasonography, transient elastography, acoustic radiation force impulse, magnetic resonance spectroscopy, magnetic resonance elastography have been employed for NASH diagnosis. Ultrasonography has shown 60-94% sensitivity and 84-95% specificity in hepatic steatosis detection (38); an acceptable first-line steatosis-screening tool in clinical practice (44) but which cannot distinguish NASH from simple steatosis (112). Transient elastography (FibroScan; Echosens, Paris, France) (113) has shown a respectable diagnostic accuracy in stratifying advanced fibrosis in NAFLD (114). However, transient elastography was found not to be useful in NASH diagnosis (115) since >10% of patients could not be assessed because of procedure failures due, mainly, to high body mass index (BMI). Hence, thresholds to define advanced fibrosis stages remain controversial. Higher scores of stiffness (kPa) to define cirrhosis are required compared to cut-offs accepted for viral hepatitis (116, 117). Magnetic resonance spectroscopy (MRS) enables the evaluation, *in vivo*, of liver molecular composition, and detects steatosis with high accuracy (118). It is the reference method for steatosis but fails in NASH detection. Magnetic resonance elastography (MRE) has been shown to be accurate in fibrosis staging (119, 120) but its availability is low in most Centres and needs further external validation. The main limitation of these image-

based methods remains their inability to detect steatohepatitis. Novel developments in the MR field, such as gadolinium probes targeted to type-1 collagen, have shown excellent preliminary results but still need to be translated into the standard clinical setting (121). The scores generated are related to the presence of steatohepatitis or fibrosis; the lower the scores, the lower the probability of suffering from steatohepatitis or significant fibrosis. The opposite is also valid i.e. the higher the score, the greater the risk of displaying steatohepatitis or significant fibrosis. Studies comparing different MRI systems manufacturers (such as Siemens vs. Phillips systems) are warranted.

The next step would be the assessment of a combination of indirect and direct markers would perform better in discriminating advanced fibrosis and NASH. The main aim is to confirm advanced fibrosis and to decide whether only to monitor patients with liver-related complications or detect which patients need in-depth hepatological evaluation, including confirmatory biopsy and experimental treatments.

Although our knowledge is constantly increasing, the number and quality of NAFLD studies are limited. Liver biopsy is currently the reference method, but it is essential to take into account the inherent limitations of this technique, such as sampling and observer variability and safety issues, that could still impair the state of ideal surrogate markers. Common non-invasive methods rely on biochemical parameters, as well as image-based approaches, but an integrated system including liver biopsy should be carried out in order to reach an increased diagnostic accuracy, enabling a more efficient and convenient management of these patients, and decreasing the required sample size of clinical trials by reducing heterogeneity in population classification. Therefore, the ultimate role of non-invasive approaches could be to guide selection of patients who require a liver biopsy to stratify disease severity and discriminate who

needs treatment. The most important aspects that should be covered are screening, diagnosis, prognosis and follow-up at variable time intervals of patients.

FibroMRI accurately predicts significant fibrosis stages. MRI can access deep tissue fibrosis staging while analysing the whole liver, and saving on sampling errors. As such, it could be useful in the management of liver donors prior to liver transplantation (122, 123). Also, it could be tested in liver diseases that share steatosis as a major feature such as, for example, viral hepatitis or alcohol-related liver diseases. Since ionizing radiation is avoided, this technique would be suitable for harmlessly monitoring fibrosis and steatohepatitis progression over time. Progression from simple steatosis to NASH and fibrosis in paired liver biopsies 3 to 6 years apart has been reported recently (4, 5). Further, in 51 patients who had undergone two liver biopsies and scored separately, the results indicated that steatosis, ballooning, inflammation and fibrosis appeared not to be equally distributed across the liver. In 21 of 51 cases there was one stage difference in the degree of fibrosis, while ballooning was detected in only one of the liver biopsies in 9 of 51 cases. As such, close follow-up of the progression of liver disease in NAFLD is mandatory, making non-invasive imaging biomarkers the optimal approach.

The main technical limitation of this technique is segmentation error because the method is based on an optical analysis of images to quantify differences not perceptible to the naked eye. The presence of vessels or different structures in the sample studied could be confounding factors resulting in under- or over-estimation of the degree of fibrosis, or inflammation. This problem can be resolved, as in the current analysis, by excluding areas containing blood vessels, biliary tract, or focal lesions and, as well, all samples with >30% pixels outside the segmented area. To avoid manual segmentation

errors, this process has been automated, thus allowing the translation of the study to different liver diseases. External validation studies are warranted.

Among the main strengths of the study is the demonstration of its applicability at different sites, and using two types of MR devices. The parameters derived from both types of machines are standardised. Further, study design was such as to minimise observer-related variation, including different measurement conditions that could impinge on diagnostic accuracy.

The expected impact and potential advantages of this method would be measured at different levels:

(i) Patient's health and quality of life improvement: These NASHMRI and FibroMRI would substitute a test requiring an invasive intervention, such as liver biopsy, by a non-invasive one that significantly reduces suffering of patients. The number of visits will be reduced as the same digital data may be used for several diagnostic techniques, improving patient comfort. Moreover, staging of the disease will allow appropriate lifestyle intervention and pharmacological treatment so that disease progression is slowed or stopped.

(ii) Patient's management: Because this method provides a global view of the whole liver, it allows better support for comparative analysis and temporal evolution studies. Archiving digital images suitable for processing will be possible providing a valuable new source of data for the professional. A new patient management algorithm will be proposed, that will allow physicians to perform life-style intervention and pharmacological treatment after detecting the histological NAFLD features with prognostic value.

(iii) Health Systems' impact: Because non-invasive it provides the ability to screen a higher number of patients at risk, rising early diagnosis and clinical efficacy. The main benefits are reduced costs (directly and indirectly through the reduction of biopsies, hospitalization days and waiting lists), improved processes, better utilization of the existing resources (MRI equipment) and improved diagnostic accuracy.

Further, it was also confirmed that NASH patients have increased hepatic mRNA expression of FGF21 and raised serum FGF21 concentration. Moreover, it was confirmed the crucial role of PNPLA3 GG-genotype in developing NASH, as well as identified a novel risk-conferring SNP, rs838133, associated with increased hazard of developing significant fibrosis. These findings are relevant, since NASH and significant fibrosis are related to a poor prognosis, and FGF21 has been recently proposed as a therapeutic target for NASH.

Finally, two novel microRNAs candidates were identified, miR-200b-3p and miR-224-5p, with a major role in NASH development. Both hepatic and plasma levels were raised in NASH patients, showing great potential as non-invasive biomarkers and hence, therapeutic targets.

FGF21 is one of the FGF family factors mainly produced by tissues with high metabolic activity, primarily liver, and has been emerged as a key regulator of glucose and lipid metabolism, playing an important role in adaptive response to endoplasmic reticulum stress (124). Liver *FGF21* mRNA expression was already found significantly increased in simple steatosis patients; nevertheless, NASH patients showed higher serum *FGF21* levels but not increased hepatic mRNA.

It has been described that exercise, and caloric restriction prevents NAFLD by reducing both mRNA *FGF21* expression and protein circulating levels in animal models (125), suggesting the potential implication of lifestyle modifications into

medium or long-term in *FGF21* expression. *In vivo* suppression of hepatic *FGF21* expression with shRNA adenovirus showed that induction of *FGF21* is required in the liver for entire regulation of its metabolism in response to a high-fat low-carbohydrate ketogenic diet on mice (126). Recently, in a cohort of aging mice that simulates the slow onset of NAFLD fed with medium-fat diet for 28 months, they observed that up-regulated *Fgf21* plasma levels were implied to be a protective response to the NAFLD-induced unfavourable outcomes (127).

FGF21 has received considerable attention due to its anti-diabetic effect in rodent models, being found paradoxically elevated in the setting of impaired glucose tolerance, together with the cluster of features presented in metabolic syndrome, such as obesity, hypertension and coronary heart disease. Additionally, plays a significant role in the pathogenic elements of NASH, through the accumulation of inactivated fatty acids, resulting in lipotoxic damage (128). These data suggest that raised *FGF21* may occur as a compensatory response to offset metabolic disturbances.

A potential role for *FGF21* in cardiovascular disease has also been pointed out. *Fgf21* knockout mice developed enhanced signs of cardiac dysfunction, and this effect was reversed *in vivo* with *FGF21* treatment (129). In agreement with animal studies, serum *FGF21* levels were increased in patients suffering from atherosclerotic disease measured by ankle-brachial index (130), and serum *FGF21* levels have also been identified as an independent risk factor for coronary artery disease (131). Finally, abnormal levels of serum FGF21 have been found associated with increased risk for all-causes and cardiovascular disease mortality (132).

In human beings, LY2405319, an *FGF21* analogue, produced significant improvements on selected metabolic disorders, such as dyslipidaemia, obesity and insulinemia, indicating that *FGF21* is bioactive in humans and could serve as a

therapeutic option (75). Furthermore, different approaches are currently investigated, such as *FGF21* conjugation with polyethylene glycol in order to increase its half-life, enhancing its anti-diabetic effects in rodents (133). Recently it was reported that simvastatin use reduces hepatic and circulating *Fgf21* levels in mice (134), and also acute exercise increases FGF21 in both serum and metabolic organs (135).

Considering that intravenous dose of *FGF21* improves insulin resistance, decreases fasting glucose and reverses steatosis in NAFLD animal models (136), increased *FGF21* gene liver expression detected in the current study, could be explained as a compensatory response to oxidative stress and glucose-lipid homeostasis disorders (62). *FGF21* could correct multiple metabolic parameters *in vitro* and *in vivo* by inducing autophagy (137) and may be part of a strategy to combat hepatic steatosis and inflammation.

In a genome-wide meta-analysis performed among 33,000 participants, rs838133 variant located in *FGF21* gene was found associated with decreased protein intake and increased carbohydrate consumption, potentially determining dietary macronutrient intake and subsequently conditioning NAFLD condition (23). Further, other four SNPs were explored in non-diabetic subjects and compared with *FGF21* protein levels, in ultrasonography NAFLD-diagnosed patients, finding an association between rs499765 and *FGF21* serum levels, and rs838133 was found associated with AST levels (138).

Consistently with these hypotheses, we found upregulation of *FGF21* at various levels, such as hepatic expression, circulating levels and increased risk of fibrosis conferred by bearing A-allele of rs838133. *FGF21* plays multiple and vital roles in regulating energy homeostasis and glucose-lipid metabolism, and currently, mechanisms that underlie this association with NAFLD are being cleared. Recently

reported data suggest that *FGF21* could be either a drug candidate with pharmacological and beneficial effects or a clinically useful biomarker for early NAFLD diagnosis, but deeper functional studies are warranted to explore further the physiological functions and regulation of *FGF21* in human beings.

Altered epigenetics patterns could distinguish between NAFLD stages, but a better understanding of the molecular mechanisms is mandatory to identify reliable biomarkers and effective treatments. Among epigenetic mechanisms, miRNAs occupy a top position, because their disturbances present potential prognostic and diagnostic, and the ability to be therapeutic targets.

Certain miRNAs are stable and easily measurable in serum or plasma and therefore hold the potential to be ideal disease biomarkers. Aberrant microRNA profiles have been previously reported in a broad spectrum of liver diseases. Promising results have been observed using circulating miRNAs as predictors of several outcomes. One of the main advantages as non-invasive biomarkers is their high stability in body fluids, enabling their use as non-invasive diagnostic and prognostic tools.

In this exploratory study, two targets were identified with potential to be non-invasive biomarkers, miR-200b-3p and miR-224-5p. Previously miR-200b has been related to hepatocellular carcinoma, acting by downregulation of the expression levels of DNA methyltransferase 3a (DNMT 3a) (139). Moreover, it has been detected an overexpression of this microRNA in tissue of primary intrahepatic cholangiocarcinoma patients, but not in plasma samples (140).

MiR-224 has also demonstrated a significant role by targeting cell proliferation, migration, invasion and anti-apoptotic properties in hepatocellular carcinoma by directly interacting with several genes (141). It has also been found overexpressed in

hepatocellular carcinoma vs normal samples (142), so different studies have been attributed it oncogenic properties, revealing that autophagy selectively regulates miR-224 expression through an autophagosome-mediated degradation system (143). Considering the tight relationship between autophagy and NASH, this could be a potential explanation of its overexpression in both liver and serum samples.

These novel results show how both microRNAs can distinguish between NASH and steatosis simple patients. The main limitation is the sample size, but a larger prospective study is now ongoing to increase the number of patients in both categories. Especially for miR-224, its plasma levels are able to accurately distinguish between both, reaching an AUROC of 0.84 in diagnosing NASH. If these results are confirmed in a larger study, this miRNA could serve as adjuncts in non-invasive diagnosis.

CONCLUSIONS

- ✓ Combined use of imaging biomarkers, NASHMRI and FibroMRI, could be useful in diagnosing steatohepatitis and significant fibrosis in patients with suspected NAFLD. Those imaging biomarkers offer clear advantages above liver biopsy since they are innocuous, less traumatic for the patient, and cheaper. Analysing the whole liver using user-friendly software would be ideal for close monitoring over time, and for extensive implementation for screening large numbers of at-risk patients. Clear disease staging on severity would provide support in clinical decision-making.

- ✓ Both hepatic and circulating levels of FGF21 were found increased in NASH, one of the most aggressive conditions of NAFLD. Further, bearing PNPLA3 GG genotype and carrying A-allele of FGF21 variant confer susceptibility to NASH and significant fibrosis development

- ✓ Two novel microRNAs were found overexpressed in NASH condition, not just in liver but also in plasma, conferring them potential as non-invasive biomarkers.

REFERENCES

1. Fargion S, Porzio M, Fracanzani AL. Nonalcoholic fatty liver disease and vascular disease: State-of-the-art. *World Journal of Gastroenterology : WJG.* 2014;20 (37):13306-24.
2. Bhala N, Angulo P, van der Poorten D, Lee E, Hui JM, Saracco G, et al. THE NATURAL HISTORY OF NONALCOHOLIC FATTY LIVER DISEASE WITH ADVANCED FIBROSIS OR CIRRHOSIS: AN INTERNATIONAL COLLABORATIVE STUDY. *Hepatology (Baltimore, Md).* 2011;54 (4):1208-16.
3. Pais R, Barritt AS, Calmus Y, Scatton O, Runge T, Lebray P, et al. NAFLD and liver transplantation: Current burden and expected challenges. *Journal of hepatology.* 2016;65 (6):1245-57.
4. Wong VW, Wong GL, Choi PC, Chan AW, Li MK, Chan HY, et al. Disease progression of non-alcoholic fatty liver disease: a prospective study with paired liver biopsies at 3 years. *Gut.* 2010;59 (7):969-74.
5. McPherson S, Hardy T, Henderson E, Burt AD, Day CP, Anstee QM. Evidence of NAFLD progression from steatosis to fibrosing-steatohepatitis using paired biopsies: implications for prognosis and clinical management. *J Hepatol.* 2015;62 (5):1148-55.
6. Adams LA, Sanderson S, Lindor KD, Angulo P. The histological course of nonalcoholic fatty liver disease: a longitudinal study of 103 patients with sequential liver biopsies. *J Hepatol.* 2005;42 (1):132-8.
7. Leslie M. The liver's weighty problem. *Science (New York, NY).* 2015;349 (6243):18-20.

8. Sanyal AJ, Banas C, Sargeant C, Luketic VA, Sterling RK, Stravitz RT, et al. Similarities and differences in outcomes of cirrhosis due to nonalcoholic steatohepatitis and hepatitis C. *Hepatology*. 2006;43 (4):682-9.
9. Hirooka M, Koizumi Y, Miyake T, Ochi H, Tokumoto Y, Tada F, et al. Nonalcoholic fatty liver disease: portal hypertension due to outflow block in patients without cirrhosis. *Radiology*. 2015;274 (2):597-604.
10. Charlton MR, Burns JM, Pedersen RA, Watt KD, Heimbach JK, Dierkhising RA. Frequency and outcomes of liver transplantation for nonalcoholic steatohepatitis in the United States. *Gastroenterology*. 2011;141 (4):1249-53.
11. Kotronen A, Yki-Jarvinen H. Fatty liver: a novel component of the metabolic syndrome. *Arteriosclerosis, thrombosis, and vascular biology*. 2008;28 (1):27-38.
12. Targher G, Day CP, Bonora E. Risk of Cardiovascular Disease in Patients with Nonalcoholic Fatty Liver Disease. *New England Journal of Medicine*. 2010;363 (14):1341-50.
13. Ampuero J, Gallego-Duran R, Romero-Gomez M. Association of NAFLD with subclinical atherosclerosis and coronary-artery disease: meta-analysis. *Revista espanola de enfermedades digestivas : organo oficial de la Sociedad Espanola de Patologia Digestiva*. 2015;107 (1):10-6.
14. Targher G, Marra F, Marchesini G. Increased risk of cardiovascular disease in non-alcoholic fatty liver disease: causal effect or epiphenomenon? *Diabetologia*. 2008;51 (11):1947-53.
15. Hermann DM, Gronewold J, Lehmann N, Seidel UK, Mohlenkamp S, Weimar C, et al. Intima-media thickness predicts stroke risk in the Heinz Nixdorf Recall study in association with vascular risk factors, age and gender. *Atherosclerosis*. 2012;224 (1):84-9.

16. Sillesen H, Muntendam P, Adourian A, Entrekin R, Garcia M, Falk E, et al. Carotid plaque burden as a measure of subclinical atherosclerosis: comparison with other tests for subclinical arterial disease in the High Risk Plaque BioImage study. *JACC Cardiovascular imaging*. 2012;5 (7):681-9.
17. Bos D, Ikram MA, Elias-Smale SE, Krestin GP, Hofman A, Witteman JC, et al. Calcification in major vessel beds relates to vascular brain disease. *Arteriosclerosis, thrombosis, and vascular biology*. 2011;31 (10):2331-7.
18. Taylor AJ, Rodriguez AE, Lee JC, Mathew SB, Cassimatis D, Gates D, et al. The relationship between subclinical atherosclerosis and electrocardiographic abnormalities as biomarkers of cardiovascular risk. *Biomarkers*. 2008;13 (5):496-504.
19. Criqui MH, McClelland RL, McDermott MM, Allison MA, Blumenthal RS, Aboyans V, et al. The ankle-brachial index and incident cardiovascular events in the MESA (Multi-Ethnic Study of Atherosclerosis). *Journal of the American College of Cardiology*. 2010;56 (18):1506-12.
20. Neuschwander-Tetri BA. Non-alcoholic fatty liver disease. *BMC Medicine*. 2017;15 (1):45.
21. Ampuero J, Ranchal I, Gallego-Duran R, Pareja MJ, Del Campo JA, Pastor-Ramirez H, et al. Oxidized low-density lipoprotein antibodies/high-density lipoprotein cholesterol ratio is linked to advanced non-alcoholic fatty liver disease lean patients. *Journal of gastroenterology and hepatology*. 2016;31 (9):1611-8.
22. Garcia-Monzon C, Lo Iacono O, Crespo J, Romero-Gomez M, Garcia-Samaniego J, Fernandez-Bermejo M, et al. Increased soluble CD36 is linked to advanced steatosis in nonalcoholic fatty liver disease. *European journal of clinical investigation*. 2014;44 (1):65-73.

23. Jurado-Ruiz E, Varela LM, Luque A, Berna G, Cahuana G, Martinez-Force E, et al. An extra virgin olive oil rich diet intervention ameliorates the nonalcoholic steatohepatitis induced by a high-fat "Western-type" diet in mice. *Molecular nutrition & food research*. 2017;61 (3).
24. Dyson JK, Anstee QM, McPherson S. Non-alcoholic fatty liver disease: a practical approach to diagnosis and staging. *Frontline Gastroenterology*. 2014;5 (3):211-8.
25. Gallego-Duran R, Ampuero J, Funuyet J, Romero-Gomez M. [Alcoholic and non-alcoholic steatohepatitis: who is affected and what can we do for them?]. *Gastroenterologia y hepatologia*. 2013;36 (9):587-96.
26. Matteoni CA, Younossi ZM, Gramlich T, Boparai N, Liu YC, McCullough AJ. Nonalcoholic fatty liver disease: a spectrum of clinical and pathological severity. *Gastroenterology*. 1999;116 (6):1413-9.
27. Brunt EM, Janney CG, Di Bisceglie AM, Neuschwander-Tetri BA, Bacon BR. Nonalcoholic steatohepatitis: a proposal for grading and staging the histological lesions. *The American journal of gastroenterology*. 1999;94 (9):2467-74.
28. Kleiner DE, Brunt EM, Van Natta M, Behling C, Contos MJ, Cummings OW, et al. Design and validation of a histological scoring system for nonalcoholic fatty liver disease. *Hepatology*. 2005;41 (6):1313-21.
29. Bedossa P. Utility and appropriateness of the fatty liver inhibition of progression (FLIP) algorithm and steatosis, activity, and fibrosis (SAF) score in the evaluation of biopsies of nonalcoholic fatty liver disease. *Hepatology*. 2014;60 (2):565-75.
30. Bedossa P, Poitou C, Veyrie N, Bouillot JL, Basdevant A, Paradis V, et al. Histopathological algorithm and scoring system for evaluation of liver lesions in morbidly obese patients. *Hepatology*. 2012;56 (5):1751-9.

31. Lackner C. Hepatocellular ballooning in nonalcoholic steatohepatitis: the pathologist's perspective. *Expert review of gastroenterology & hepatology*. 2011;5 (2):223-31.
32. Ratziu V, Charlotte F, Heurtier A, Gombert S, Giral P, Bruckert E, et al. Sampling variability of liver biopsy in nonalcoholic fatty liver disease. *Gastroenterology*. 2005;128 (7):1898-906.
33. Ekstedt M, Hagstrom H, Nasr P, Fredrikson M, Stal P, Kechagias S, et al. Fibrosis stage is the strongest predictor for disease-specific mortality in NAFLD after up to 33 years of follow-up. *Hepatology*. 2015;61 (5):1547-54.
34. Angulo P, Kleiner DE, Dam-Larsen S, Adams LA, Bjornsson ES, Charatcharoenwitthaya P, et al. Liver Fibrosis, but No Other Histologic Features, Is Associated With Long-term Outcomes of Patients With Nonalcoholic Fatty Liver Disease. *Gastroenterology*. 2015;149 (2):389-97.e10.
35. Biomarkers and surrogate endpoints: preferred definitions and conceptual framework. *Clinical pharmacology and therapeutics*. 2001;69 (3):89-95.
36. EASL-EASD-EASO Clinical Practice Guidelines for the management of non-alcoholic fatty liver disease. *J Hepatol*. 2016;64.
37. Hamer OW, Aguirre DA, Casola G, Lavine JE, Woenckhaus M, Sirlin CB. Fatty Liver: Imaging Patterns and Pitfalls. *RadioGraphics*. 2006;26 (6):1637-53.
38. Schwenzer NF, Springer F, Schraml C, Stefan N, Machann J, Schick F. Non-invasive assessment and quantification of liver steatosis by ultrasound, computed tomography and magnetic resonance. *J Hepatol*. 2009;51 (3):433-45.
39. Saadeh S, Younossi ZM, Remer EM, Gramlich T, Ong JP, Hurley M, et al. The utility of radiological imaging in nonalcoholic fatty liver disease. *Gastroenterology*. 2002;123 (3):745-50.

40. Dulai PS, Sirlin CB, Loomba R. MRI and MRE for non-invasive quantitative assessment of hepatic steatosis and fibrosis in NAFLD and NASH: Clinical trials to clinical practice. *J Hepatol.* 2016;65 (5):1006-16.
41. Jimenez-Aguero R, Emparanza JI, Beguiristain A, Bujanda L, Alustiza JM, Garcia E, et al. Novel equation to determine the hepatic triglyceride concentration in humans by MRI: diagnosis and monitoring of NAFLD in obese patients before and after bariatric surgery. *BMC Med.* 2014;12:137.
42. Singh S, Venkatesh SK, Loomba R, Wang Z, Sirlin C, Chen J, et al. Magnetic resonance elastography for staging liver fibrosis in non-alcoholic fatty liver disease: a diagnostic accuracy systematic review and individual participant data pooled analysis. *European radiology.* 2016;26 (5):1431-40.
43. Park CC, Nguyen P, Hernandez C, Bettencourt R, Ramirez K, Fortney L, et al. Magnetic Resonance Elastography vs Transient Elastography in Detection of Fibrosis and Noninvasive Measurement of Steatosis in Patients With Biopsy-Proven Nonalcoholic Fatty Liver Disease. *Gastroenterology.* 2017;152 (3):598-607.e2.
44. Castera L, Vilgrain V, Angulo P. Noninvasive evaluation of NAFLD. *Nat Rev Gastroenterol Hepatol.* 2013;10 (11):666-75.
45. Moon CM, Oh CH, Ahn KY, Yang JS, Kim JY, Shin SS, et al. Metabolic biomarkers for non-alcoholic fatty liver disease induced by high-fat diet: In vivo magnetic resonance spectroscopy of hyperpolarized [1-13C] pyruvate. *Biochemical and biophysical research communications.* 2017;482 (1):112-9.
46. Boursier J, Vergniol J, Guillet A, Hiriart JB, Lannes A, Bail B, et al. Diagnostic accuracy and prognostic significance of blood fibrosis tests and liver stiffness measurement by FibroScan in non-alcoholic fatty liver disease. *J Hepatol.* 2016;65.

47. Petta S, Maida M, Macaluso FS, Di Marco V, Camma C, Cabibi D, et al. The severity of steatosis influences liver stiffness measurement in patients with nonalcoholic fatty liver disease. *Hepatology*. 2015;62 (4):1101-10.
48. Yoneda M, Yoneda M, Mawatari H, Fujita K, Endo H, Iida H, et al. Noninvasive assessment of liver fibrosis by measurement of stiffness in patients with nonalcoholic fatty liver disease (NAFLD). *Digestive and liver disease : official journal of the Italian Society of Gastroenterology and the Italian Association for the Study of the Liver*. 2008;40 (5):371-8.
49. Mahadeva S, Mahfudz AS, Vijayanathan A, Goh KL, Kulenthiran A, Cheah PL. Performance of transient elastography (TE) and factors associated with discordance in non-alcoholic fatty liver disease. *Journal of digestive diseases*. 2013;14 (11):604-10.
50. Yoshioka K, Hashimoto S, Kawabe N. Measurement of liver stiffness as a non-invasive method for diagnosis of non-alcoholic fatty liver disease. *Hepatology research : the official journal of the Japan Society of Hepatology*. 2015;45 (2):142-51.
51. Myers RP, Pomier-Layrargues G, Kirsch R, Pollett A, Duarte-Rojo A, Wong D, et al. Feasibility and diagnostic performance of the FibroScan XL probe for liver stiffness measurement in overweight and obese patients. *Hepatology*. 2012;55 (1):199-208.
52. Petta S, Wai-Sun Wong V, Camma C, Hiriart JB, Wong GL, Marra F, et al. Improved Noninvasive prediction of Liver Fibrosis by Liver Stiffness Measurement in Patients with Nonalcoholic Fatty Liver Disease Accounting for Controlled Attenuation Parameter Values. *Hepatology*. 2016.
53. Imajo K, Kessoku T, Honda Y, Tomeno W, Ogawa Y, Mawatari H, et al. Magnetic Resonance Imaging More Accurately Classifies Steatosis and Fibrosis in

Patients With Nonalcoholic Fatty Liver Disease Than Transient Elastography. *Gastroenterology*. 2016;150 (3):626-37.e7.

54. Romero-Gómez M, Cortez-Pinto H. Detecting liver fat from viscoelasticity: How good is CAP in clinical practice? The need for universal cut-offs. *Journal of Hepatology*.

55. Palmeri ML, Wang MH, Rouze NC, Abdelmalek MF, Guy CD, Moser B, et al. Noninvasive evaluation of hepatic fibrosis using acoustic radiation force-based shear stiffness in patients with nonalcoholic fatty liver disease. *J Hepatol*. 2011;55 (3):666-72.

56. Yoneda M, Suzuki K, Kato S, Fujita K, Nozaki Y, Hosono K, et al. Nonalcoholic fatty liver disease: US-based acoustic radiation force impulse elastography. *Radiology*. 2010;256 (2):640-7.

57. Guzman-Aroca F, Frutos-Bernal MD, Bas A, Lujan-Mompean JA, Reus M, Berna-Serna Jde D, et al. Detection of non-alcoholic steatohepatitis in patients with morbid obesity before bariatric surgery: preliminary evaluation with acoustic radiation force impulse imaging. *European radiology*. 2012;22 (11):2525-32.

58. Fierbinteanu Braticевичi C, Sporea I, Panaitescu E, Tribus L. Value of acoustic radiation force impulse imaging elastography for non-invasive evaluation of patients with nonalcoholic fatty liver disease. *Ultrasound in medicine & biology*. 2013;39 (11):1942-50.

59. Feldstein AE, Wieckowska A, Lopez AR, Liu YC, Zein NN, McCullough AJ. Cytokeratin-18 fragment levels as noninvasive biomarkers for nonalcoholic steatohepatitis: a multicenter validation study. *Hepatology*. 2009;50 (4):1072-8.

60. Yang M, Xu D, Liu Y, Guo X, Li W, Guo C, et al. Combined Serum Biomarkers in Non-Invasive Diagnosis of Non-Alcoholic Steatohepatitis. *PloS one*. 2015;10 (6):e0131664.

61. Cusi K, Chang Z, Harrison S, Lomonaco R, Bril F, Orsak B, et al. Limited value of plasma cytokeratin-18 as a biomarker for NASH and fibrosis in patients with non-alcoholic fatty liver disease. *J Hepatol.* 2014;60 (1):167-74.
62. Liu J, Xu Y, Hu Y, Wang G. The role of fibroblast growth factor 21 in the pathogenesis of non-alcoholic fatty liver disease and implications for therapy. *Metabolism.* 2015;64 (3):380-90.
63. Woo YC, Xu A, Wang Y, Lam KS. Fibroblast growth factor 21 as an emerging metabolic regulator: clinical perspectives. *Clinical endocrinology.* 2013;78 (4):489-96.
64. von Holstein-Rathlou S, BonDurant Lucas D, Peltekian L, Naber Meghan C, Yin Terry C, Claflin Kristin E, et al. FGF21 Mediates Endocrine Control of Simple Sugar Intake and Sweet Taste Preference by the Liver. *Cell Metabolism.* 23 (2):335-43.
65. Kharitononkov A, Wroblewski VJ, Koester A, Chen YF, Clutinger CK, Tigno XT, et al. The metabolic state of diabetic monkeys is regulated by fibroblast growth factor-21. *Endocrinology.* 2007;148 (2):774-81.
66. Huang X, Yu C, Jin C, Yang C, Xie R, Cao D, et al. Forced expression of hepatocyte-specific fibroblast growth factor 21 delays initiation of chemically induced hepatocarcinogenesis. *Molecular carcinogenesis.* 2006;45 (12):934-42.
67. Novotny D, Vaverkova H, Karasek D, Lukes J, Slavik L, Malina P, et al. Evaluation of total adiponectin, adipocyte fatty acid binding protein and fibroblast growth factor 21 levels in individuals with metabolic syndrome. *Physiological research.* 2014;63 (2):219-28.
68. Cheung BM, Deng HB. Fibroblast growth factor 21: a promising therapeutic target in obesity-related diseases. *Expert review of cardiovascular therapy.* 2014;12 (6):659-66.

69. Li X, Fan X, Ren F, Zhang Y, Shen C, Ren G, et al. Serum FGF21 levels are increased in newly diagnosed type 2 diabetes with nonalcoholic fatty liver disease and associated with hsCRP levels independently. *Diabetes research and clinical practice*. 2011;93 (1):10-6.
70. Lee Y, Lim S, Hong ES, Kim JH, Moon MK, Chun EJ, et al. Serum FGF21 concentration is associated with hypertriglyceridaemia, hyperinsulinaemia and pericardial fat accumulation, independently of obesity, but not with current coronary artery status. *Clinical endocrinology*. 2014;80 (1):57-64.
71. Li H, Fang Q, Gao F, Fan J, Zhou J, Wang X, et al. Fibroblast growth factor 21 levels are increased in nonalcoholic fatty liver disease patients and are correlated with hepatic triglyceride. *J Hepatol*. 2010;53 (5):934-40.
72. Yilmaz Y, Eren F, Yonal O, Kurt R, Aktas B, Celikel CA, et al. Increased serum FGF21 levels in patients with nonalcoholic fatty liver disease. *European journal of clinical investigation*. 2010;40 (10):887-92.
73. Dushay J, Chui PC, Gopalakrishnan GS, Varela-Rey M, Crawley M, Fisher FM, et al. Increased fibroblast growth factor 21 in obesity and nonalcoholic fatty liver disease. *Gastroenterology*. 2010;139 (2):456-63.
74. Fisher FM, Chui PC, Antonellis PJ, Bina HA, Kharitononkov A, Flier JS, et al. Obesity is a fibroblast growth factor 21 (FGF21)-resistant state. *Diabetes*. 2010;59 (11):2781-9.
75. Gaich G, Chien JY, Fu H, Glass LC, Deeg MA, Holland WL, et al. The effects of LY2405319, an FGF21 analog, in obese human subjects with type 2 diabetes. *Cell Metab*. 2013;18 (3):333-40.

76. Chu AY, Workalemahu T, Paynter NP, Rose LM, Giulianini F, Tanaka T, et al. Novel locus including FGF21 is associated with dietary macronutrient intake. *Human molecular genetics*. 2013;22 (9):1895-902.
77. Angulo P, Hui JM, Marchesini G, Bugianesi E, George J, Farrell GC, et al. The NAFLD fibrosis score: a noninvasive system that identifies liver fibrosis in patients with NAFLD. *Hepatology*. 2007;45 (4):846-54.
78. Musso G, Cassader M, Gambino R. Non-alcoholic steatohepatitis: emerging molecular targets and therapeutic strategies. *Nat Rev Drug Discov*. 2016;15.
79. Takahashi Y, Kurosaki M, Tamaki N, Yasui Y, Hosokawa T, Tsuchiya K, et al. Non-alcoholic fatty liver disease fibrosis score and FIB-4 scoring system could identify patients at risk of systemic complications. *Hepatology research : the official journal of the Japan Society of Hepatology*. 2015;45 (6):667-75.
80. Cales P, Laine F, Boursier J, Deugnier Y, Moal V, Oberti F, et al. Comparison of blood tests for liver fibrosis specific or not to NAFLD. *J Hepatol*. 2009;50 (1):165-73.
81. Wai CT, Greenson JK, Fontana RJ, Kalbfleisch JD, Marrero JA, Conjeevaram HS, et al. A simple noninvasive index can predict both significant fibrosis and cirrhosis in patients with chronic hepatitis C. *Hepatology*. 2003;38 (2):518-26.
82. Forns X, Ampurdanes S, Llovet JM, Aponte J, Quinto L, Martinez-Bauer E, et al. Identification of chronic hepatitis C patients without hepatic fibrosis by a simple predictive model. *Hepatology*. 2002;36 (4 Pt 1):986-92.
83. Lykiardopoulos B, Hagström H, Fredrikson M, Ignatova S, Stål P, Hulcrantz R, et al. Development of Serum Marker Models to Increase Diagnostic Accuracy of Advanced Fibrosis in Nonalcoholic Fatty Liver Disease: The New LINKI Algorithm Compared with Established Algorithms. *PloS one*. 2016;11 (12):e0167776.

84. Shah AG, Lydecker A, Murray K, Tetri BN, Contos MJ, Sanyal AJ. Comparison of noninvasive markers of fibrosis in patients with nonalcoholic fatty liver disease. *Clin Gastroenterol Hepatol*. 2009;7 (10):1104-12.
85. Romera M, Corpas R, Romero Gomez M. Insulin resistance as a non-invasive method for the assessment of fibrosis in patients with hepatitis C: a comparative study of biochemical methods. *Revista espanola de enfermedades digestivas : organo oficial de la Sociedad Espanola de Patologia Digestiva*. 2006;98 (3):161-9.
86. Harrison SA, Oliver D, Arnold HL, Gogia S, Neuschwander-Tetri BA. Development and validation of a simple NAFLD clinical scoring system for identifying patients without advanced disease. *Gut*. 2008;57 (10):1441-7.
87. Nassif AT, Nagano TA, Okayama S, Nassif LS, Branco Filho A, Sampaio Neto J. Performance of the Bard Scoring System in Bariatric Surgery Patients with Nonalcoholic Fatty Liver Disease. *Obesity surgery*. 2017;27 (2):394-8.
88. Morra R, Munteanu M, Imbert-Bismut F, Messous D, Ratziu V, Poynard T. FibroMAX: towards a new universal biomarker of liver disease? Expert review of molecular diagnostics. 2007;7 (5):481-90.
89. Fouad A, Sabry D, Ahmed R, Kamal M, Allah SA, Marzouk S, et al. Comparative diagnostic study of biomarkers using FibroMax and pathology for prediction of liver steatosis in patients with chronic hepatitis C virus infection: an Egyptian study. *International journal of general medicine*. 2013;6:127-34.
90. Grattagliano I, Ubaldi E, Napoli L, Marulli CF, Nebiacolombo C, Cottone C, et al. Utility of noninvasive methods for the characterization of nonalcoholic liver steatosis in the family practice. The "VARES" Italian multicenter study. *Annals of hepatology*. 2013;12 (1):70-7.

91. Perazzo H, Munteanu M, Ngo Y, Lebray P, Seurat N, Rutka F, et al. Prognostic value of liver fibrosis and steatosis biomarkers in type-2 diabetes and dyslipidaemia. *Aliment Pharmacol Ther.* 2014;40 (9):1081-93.
92. Munteanu M, Tiniakos D, Anstee Q, Charlotte F, Marchesini G, Bugianesi E, et al. Diagnostic performance of FibroTest, SteatoTest and ActiTest in patients with NAFLD using the SAF score as histological reference. *Alimentary Pharmacology & Therapeutics.* 2016;44 (8):877-89.
93. Barr J, Caballeria J, Martinez-Arranz I, Dominguez-Diez A, Alonso C, Muntane J, et al. Obesity-dependent metabolic signatures associated with nonalcoholic fatty liver disease progression. *Journal of proteome research.* 2012;11 (4):2521-32.
94. EASL-ALEH Clinical Practice Guidelines: Non-invasive tests for evaluation of liver disease severity and prognosis. *J Hepatol.* 2015;63 (1):237-64.
95. Struben VM, Hespeneide EE, Caldwell SH. Nonalcoholic steatohepatitis and cryptogenic cirrhosis within kindreds. *The American journal of medicine.* 2000;108 (1):9-13.
96. Loomba R, Schork N, Chen CH, Bettencourt R, Bhatt A, Ang B, et al. Heritability of Hepatic Fibrosis and Steatosis Based on a Prospective Twin Study. *Gastroenterology.* 2015;149 (7):1784-93.
97. Romeo S, Kozlitina J, Xing C, Pertsemlidis A, Cox D, Pennacchio LA, et al. Genetic variation in PNPLA3 confers susceptibility to nonalcoholic fatty liver disease. *Nature genetics.* 2008;40 (12):1461-5.
98. Valenti L, Al-Serri A, Daly AK, Galmozzi E, Rametta R, Dongiovanni P, et al. Homozygosity for the patatin-like phospholipase-3/adiponutrin I148M polymorphism influences liver fibrosis in patients with nonalcoholic fatty liver disease. *Hepatology.* 2010;51 (4):1209-17.

99. Shen J, Wong GL, Chan HL, Chan RS, Chan HY, Chu WC, et al. PNPLA3 gene polymorphism and response to lifestyle modification in patients with nonalcoholic fatty liver disease. *Journal of gastroenterology and hepatology*. 2015;30 (1):139-46.
100. Kozlitina J, Smagris E, Stender S, Nordestgaard BG, Zhou HH, Tybjaerg-Hansen A, et al. Exome-wide association study identifies a TM6SF2 variant that confers susceptibility to nonalcoholic fatty liver disease. *Nature genetics*. 2014;46 (4):352-6.
101. Liu YL, Reeves HL, Burt AD, Tiniakos D, McPherson S, Leathart JB, et al. TM6SF2 rs58542926 influences hepatic fibrosis progression in patients with non-alcoholic fatty liver disease. *Nature communications*. 2014;5:4309.
102. Dongiovanni P, Petta S, Maglio C, Fracanzani AL, Pipitone R, Mozzi E, et al. Transmembrane 6 superfamily member 2 gene variant disentangles nonalcoholic steatohepatitis from cardiovascular disease. *Hepatology*. 2015;61 (2):506-14.
103. Gallego-Duran R, Romero-Gomez M. Epigenetic mechanisms in non-alcoholic fatty liver disease: An emerging field. *World journal of hepatology*. 2015;7 (24):2497-502.
104. Executive Summary of The Third Report of The National Cholesterol Education Program (NCEP) Expert Panel on Detection, Evaluation, And Treatment of High Blood Cholesterol In Adults (Adult Treatment Panel III). *Jama*. 2001;285 (19):2486-97.
105. Sud A, Hui JM, Farrell GC, Bandara P, Kench JG, Fung C, et al. Improved prediction of fibrosis in chronic hepatitis C using measures of insulin resistance in a probability index. *Hepatology*. 2004;39 (5):1239-47.
106. Ginzinger DG. Gene quantification using real-time quantitative PCR: an emerging technology hits the mainstream. *Experimental hematology*. 2002;30 (6):503-12.

107. Hanley JA, McNeil BJ. A method of comparing the areas under receiver operating characteristic curves derived from the same cases. *Radiology*. 1983;148(3):839-43.
108. Tom T. *ROC Graphs: Notes and Practical Considerations for Researchers*. 2004.
109. Zhang E, Wartelle-Bladou C, Lepanto L, Lachaine J, Cloutier G, Tang A. Cost-utility analysis of nonalcoholic steatohepatitis screening. *European radiology*. 2015;25(11):3282-94.
110. Munteanu M, Ratziu V, Morra R, Messous D, Imbert-Bismut F, Poynard T. Noninvasive biomarkers for the screening of fibrosis, steatosis and steatohepatitis in patients with metabolic risk factors: FibroTest-FibroMax experience. *Journal of gastrointestinal and liver diseases : JGLD*. 2008;17(2):187-91.
111. Barr J, Vazquez-Chantada M, Alonso C, Perez-Cormenzana M, Mayo R, Galan A, et al. Liquid chromatography-mass spectrometry-based parallel metabolic profiling of human and mouse model serum reveals putative biomarkers associated with the progression of nonalcoholic fatty liver disease. *Journal of proteome research*. 2010;9(9):4501-12.
112. Hernaez R, Lazo M, Bonekamp S, Kamel I, Brancati FL, Guallar E, et al. Diagnostic accuracy and reliability of ultrasonography for the detection of fatty liver: a meta-analysis. *Hepatology*. 2011;54(3):1082-90.
113. Sandrin L, Fourquet B, Hasquenoph JM, Yon S, Fournier C, Mal F, et al. Transient elastography: a new noninvasive method for assessment of hepatic fibrosis. *Ultrasound in medicine & biology*. 2003;29(12):1705-13.
114. de Ledingham V, Wong VW, Vergniol J, Wong GL, Foucher J, Chu SH, et al. Diagnosis of liver fibrosis and cirrhosis using liver stiffness measurement: comparison between M and XL probe of FibroScan (R). *J Hepatol*. 2012;56(4):833-9.

115. Kumar R, Rastogi A, Sharma MK, Bhatia V, Tyagi P, Sharma P, et al. Liver stiffness measurements in patients with different stages of nonalcoholic fatty liver disease: diagnostic performance and clinicopathological correlation. *Dig Dis Sci.* 2013;58 (1):265-74.
116. Myers RP, Pomier-Layrargues G, Kirsch R, Pollett A, Beaton M, Levstik M, et al. Discordance in fibrosis staging between liver biopsy and transient elastography using the FibroScan XL probe. *J Hepatol.* 2012;56 (3):564-70.
117. Kwok R, Tse YK, Wong GL, Ha Y, Lee AU, Ngu MC, et al. Systematic review with meta-analysis: non-invasive assessment of non-alcoholic fatty liver disease--the role of transient elastography and plasma cytokeratin-18 fragments. *Aliment Pharmacol Ther.* 2014;39 (3):254-69.
118. Ligabue G, Besutti G, Scaglioni R, Stentarelli C, Guaraldi G. MR quantitative biomarkers of non-alcoholic fatty liver disease: technical evolutions and future trends. *Quantitative Imaging in Medicine and Surgery.* 2013;3 (4):192-5.
119. Kim D, Kim WR, Talwalkar JA, Kim HJ, Ehman RL. Advanced fibrosis in nonalcoholic fatty liver disease: noninvasive assessment with MR elastography. *Radiology.* 2013;268 (2):411-9.
120. Orlacchio A, Bolacchi F, Antonicoli M, Coco I, Costanzo E, Tosti D, et al. Liver Elasticity in NASH Patients Evaluated with Real-Time Elastography (RTE). *Ultrasound in medicine & biology.* 2012;38 (4):537-44.
121. Fuchs BC, Wang H, Yang Y, Wei L, Polasek M, Schuhle DT, et al. Molecular MRI of collagen to diagnose and stage liver fibrosis. *J Hepatol.* 2013;59 (5):992-8.
122. Marsman H, Matsushita T, Dierkhising R, Kremers W, Rosen C, Burgart L, et al. Assessment of donor liver steatosis: pathologist or automated software? *Human pathology.* 2004;35 (4):430-5.

123. Markin RS, Wisecarver JL, Radio SJ, Stratta RJ, Langnas AN, Hirst K, et al. Frozen section evaluation of donor livers before transplantation. *Transplantation*. 1993;56 (6):1403-9.
124. Kim SH, Kim KH, Kim HK, Kim MJ, Back SH, Konishi M, et al. Fibroblast growth factor 21 participates in adaptation to endoplasmic reticulum stress and attenuates obesity-induced hepatic metabolic stress. *Diabetologia*. 2015;58 (4):809-18.
125. Fletcher JA, Meers GM, Laughlin MH, Ibdah JA, Thyfault JP, Rector RS. Modulating fibroblast growth factor 21 in hyperphagic OLETF rats with daily exercise and caloric restriction. *Applied physiology, nutrition, and metabolism = Physiologie appliquee, nutrition et metabolisme*. 2012;37 (6):1054-62.
126. Badman MK, Pissios P, Kennedy AR, Koukos G, Flier JS, Maratos-Flier E. Hepatic fibroblast growth factor 21 is regulated by PPARalpha and is a key mediator of hepatic lipid metabolism in ketotic states. *Cell Metab*. 2007;5 (6):426-37.
127. Rusli F, Deelen J, Andriyani E, Boekschoten MV, Lute C, van den Akker EB, et al. Fibroblast growth factor 21 reflects liver fat accumulation and dysregulation of signalling pathways in the liver of C57BL/6J mice. *Scientific Reports*. 2016;6.
128. Fisher FM, Chui PC, Nasser IA, Popov Y, Cunniff JC, Lundasen T, et al. Fibroblast growth factor 21 limits lipotoxicity by promoting hepatic fatty acid activation in mice on methionine and choline-deficient diets. *Gastroenterology*. 2014;147 (5):1073-83.e6.
129. Planavila A, Redondo-Angulo I, Ribas F, Garrabou G, Casademont J, Giralt M, et al. Fibroblast growth factor 21 protects the heart from oxidative stress. *Cardiovascular research*. 2015;106 (1):19-31.

130. Zhang X, Hu Y, Zeng H, Li L, Zhao J, Zhao J, et al. Serum fibroblast growth factor 21 levels is associated with lower extremity atherosclerotic disease in Chinese female diabetic patients. *Cardiovascular Diabetology*. 2015;14.
131. Shen Y, Ma X, Zhou J, Pan X, Hao Y, Zhou M, et al. Additive relationship between serum fibroblast growth factor 21 level and coronary artery disease. *Cardiovascular Diabetology*. 2013;12:124.
132. Li Q, Zhang Y, Ding D, Yang Y, Chen Q, Su D, et al. Association Between Serum Fibroblast Growth Factor 21 and Mortality Among Patients With Coronary Artery Disease. *The Journal of clinical endocrinology and metabolism*. 2016;101(12):4886-94.
133. Song L, Zhu Y, Wang H, Belov AA, Niu J, Shi L, et al. A solid-phase PEGylation strategy for protein therapeutics using a potent FGF21 analog. *Biomaterials*. 2014;35(19):5206-15.
134. Ziros P, Zagoriti Z, Lagoumintzis G, Kyriazopoulou V, Iskrenova RP, Habeos EI, et al. Hepatic Fgf21 Expression Is Repressed after Simvastatin Treatment in Mice. *PloS one*. 2016;11(9):e0162024.
135. Tanimura Y, Aoi W, Takanami Y, Kawai Y, Mizushima K, Naito Y, et al. Acute exercise increases fibroblast growth factor 21 in metabolic organs and circulation. *Physiological Reports*. 2016;4(12).
136. Kim HW, Lee JE, Cha JJ, Hyun YY, Kim JE, Lee MH, et al. Fibroblast growth factor 21 improves insulin resistance and ameliorates renal injury in db/db mice. *Endocrinology*. 2013;154(9):3366-76.
137. Zhu S, Wu Y, Ye X, Ma L, Qi J, Yu D, et al. FGF21 ameliorates nonalcoholic fatty liver disease by inducing autophagy. *Molecular and cellular biochemistry*. 2016;420(1-2):107-19.

138. Jiang S, Zhang R, Li H, Fang Q, Jiang F, Hou X, et al. The single nucleotide polymorphism rs499765 is associated with fibroblast growth factor 21 and nonalcoholic fatty liver disease in a Chinese population with normal glucose tolerance. *Journal of nutrigenetics and nutrigenomics*. 2014;7 (3):121-9.
139. Li XY, Feng XZ, Tang JZ, Dong K, Wang JF, Meng CC, et al. MicroRNA-200b inhibits the proliferation of hepatocellular carcinoma by targeting DNA methyltransferase 3a. *Molecular medicine reports*. 2016;13 (5):3929-35.
140. Correa-Gallego C, Maddalo D, Doussot A, Kemeny N, Kingham TP, Allen PJ, et al. Circulating Plasma Levels of MicroRNA-21 and MicroRNA-221 Are Potential Diagnostic Markers for Primary Intrahepatic Cholangiocarcinoma. *PloS one*. 2016;11 (9):e0163699.
141. Zhang Y, Takahashi S, Tasaka A, Yoshima T, Ochi H, Chayama K. Involvement of microRNA-224 in cell proliferation, migration, invasion, and anti-apoptosis in hepatocellular carcinoma. *Journal of gastroenterology and hepatology*. 2013;28 (3):565-75.
142. He TL, Zheng KL, Li G, Song B, Zhang YJ. Identification of typical miRNAs and target genes in hepatocellular carcinoma by DNA microarray technique. *European review for medical and pharmacological sciences*. 2014;18 (1):108-16.
143. Lan SH, Wu SY, Zuchini R, Lin XZ, Su IJ, Tsai TF, et al. Autophagy-preferential degradation of MIR224 participates in hepatocellular carcinoma tumorigenesis. *Autophagy*. 2014;10 (9):1687-9.
-

